# TRACER TRANSPORT ON THE EASTERN FLANK OF THE JUAN DE FUCA RIDGE

## A THESIS SUBMITTED TO THE GLOBAL ENVIRONMENTAL SCIENCE UNDERGRADUATE DIVISION IN PARTIAL FULFILLMENT OF THE REQUIREMENTS FOR THE DEGREE OF

## BACHELOR OF SCIENCE

## IN

## GLOBAL ENVIRONMENTAL SCIENCE

## DECEMBER 2012

By
Jordan Guss

Thesis Advisor
Dr. James Cowen

I certify that I have read this thesis and that, in my opinion, it is

satisfactory in scope and quality as a thesis for the degree of Bachelor of

Science in Global Environmental Science.

**THESIS ADVISOR**

_____
____

**Dr. James Cowen**
**Department of Oceanography**

# ACKNOWLEDGEMENTS

# ABSTRACT

Much of the ocean floor is hydrogeologically active, but little is known about the physical properties of oceanic crust. Here is a description of the instrumentation and methodology used to obtain a quantitative assessment of the hydrological properties of the upper ocean crust on the eastern flank of the Juan de Fuca Ridge; preliminary results are also included and discussed. Many tracers were pumped into the upper basement around Hole U1362B during Integrated Ocean Drilling Program (IODP) Expedition 327 as part of a single and cross hole tracer experiment on the eastern flank of the Juan de Fuca Ridge. This paper focuses on the use of fluorescence microspheres as synthetic tracers of hydrologic transport. The aim of this 24-hour pumping experiment was to test a large volume of basement rock around Hole U1362B. This paper reports on the design of the tracer experiment, the methods used to prepare and inject the tracers (using shipboard mud and cement pump systems), and the tools developed to permit shipboard and downhole sampling of injectate fluid. Onshore analysis of the raw injection samples (pre-injection into basement) is essential for interpretation of long-term samples collected from subseafloor borehole observatories ("CORKs"). Borehole samples were continuously collected within a long-term CORK installed in Hole U1362B after the tracer injection was completed. Although the arrival of microspheres at collection site U1301A was not yet detected, the vast decrease in microsphere concentration at injection site U1362B in the 11 months following injection indicate that the microspheres are being transported elsewhere. This paper also addresses some possible explanations for this decrease in concentration and the future research needed to provide a more thorough quantitative assessment of tracer transport behavior in the upper ocean crust.

**TABLE OF CONTENTS**

# LIST OF TABLES

# LIST OF FIGURES

# CHAPTER I
# INTRODUCTION

## 1.0    Introduction

The presence of freshwater aquifers in continental crust has been known for thousands of years: since humans dug the first well.  In the past several decades, however, it has been found that there is another major fluid reservoir located in the subseafloor oceanic crust, but very little is known about the fluid stored within the ocean crust.  The flow of this fluid within the oceans' volcanic crust influences the temperature and chemical state of these fluids, as well as the transport of solutes; the crustal fluid flow also affects the formation and maintenance of microbial communities below the seafloor (Alt, 1995; Cowen et al., 2003; Cowen 2004; Huber et al., 2006; Parsons and Sclater, 1977; Peacock and Wang, 1999).  The flux of these crustal fluids on a global scale is comparable to the world's rivers' input into the oceans.  It is estimated that once every $10^5 - 10^6$ years, a volume equal to all the world's oceans passes through the crust (Elderfield and Schultz, 1996; Johnson and Pruis, 2003; Mottl, 2003).

Currently, there is little information available regarding the actual paths of large-scale fluid transport flow in the oceanic crust.  While the crust is often thought of as a layer whose properties smoothly vary with changes in depth, core samples and wireline logs from boreholes suggest that the pathways for crustal fluid flow are extremely complex (Bach et. al., 2004; Bartetzko, 2005; Gillis and Robinson, 1990; Gillis et. al., 2001; Karson, 1998).

## 1.1 Ocean Basement Environment

The ocean floor comprises approximately two thirds of the Earth's surface. Partially covered by a thick layer of sediment, the subseafloor basement rock is a vast, largely unexplored environment (Cowen et al., 2003; Cowen 2004). It has been shown that the majority of the oceanic basement floor is hydrogeologically active (Davis and Elderfield, 2004). Many tracer transport experiments have been carried out to determine rates and directions of crustal fluid flow in continental aquifers (Becker et al., 2003; Close et al., 2006), yet a tracer transport experiment had never before been implemented in an oceanic crustal setting until recently (Fisher et al. 2011).

The volcanic oceanic basement is estimated to contain a volume of water comparable to that of the ice caps and glaciers combined, making it the largest aquifer in the world (Johnson and Pruis, 2003). Recently, scientific ocean floor drilling focused much of its attention to "ridge flank" areas. These are areas where sediments help to improve the stability of the drill string, and the conditions of the basement environment make experimentation and sampling a more practical endeavor (Cowen, 2006). Verifying that two different crustal sites hundreds of meters apart are connected in a hydrologic manner, as well as determining the time needed for tracers to travel between the sites, would be great achievements in the scope of the tracer transport experiment described in this paper (Fisher et al., 2011).

The setting of this particular experiment is the eastern flank of the Juan de Fuca Ridge, a seafloor spreading center located off the northwest coast of North America. This area of the seafloor is an ideal location for scientific ocean floor drilling. During the Pleistocene, the region was subject to high rates of sedimentation, which buried much of

the basement rock at a relatively young age (Davis et al., 1997; Underwood et al., 2005). Because the ocean crust in this region of the Juan de Fuca Ridge was buried at such a young age, scientists are able to study younger ocean basement than would be possible elsewhere. The sediment also has low permeability, which minimizes heat loss from most of the ridge flank. This provides the basement with strong thermal and chemical gradients.

## 1.2 Tracer Transport Project

The aim of the Tracer Transport Project was to obtain fundamental qualitative and quantitative information about transport of crustal fluids in the eastern flank of the Juan de Fuca Ridge. The desired results include the rates and directions of fluid and particle transport, the relationship between particle transport and solute transport, the permeability of the crust, and the vertical and horizontal connectivity between ocean crust boreholes (Fisher et al., 2011).

For years, scientific ocean drilling has been in pursuit of a quantitative assessment of the dynamics and impacts of the crustal fluid flow through the ocean basement (Working Group 3, 1987). Advances in drilling technology were required to address questions pertaining to the underexplored deep biosphere. With the recent development of pressure-tight subseafloor observatories, scientists have marked a great step forward in the progress of hydrogeologic instrumentation (Davis et al., 1992; Davis and Becker, 2002). These observatories (Circulation Obviation Retrofit Kits, or "CORKs") offered unprecedented opportunities to study biogeochemical properties and microbial diversity in deep, sediment-buried oceanic crust environments. CORKs are capable of in-situ fluid

sampling, automated temperature and pressure data collection and logging, and they are also used as long-term sites for sampling and monitoring. Seafloor drilling is a violent endeavor, and it disrupts the natural state of the subseafloor environment with chemical and thermal disturbances. Because CORKs are long-term monitoring and sampling sites, they are capable of permitting the various disturbances associated with drilling (thermal, pressure, chemical) to dissipate with time, allowing the environment around the drill site to equilibrate and return to pre-drilling, natural conditions. This provides the ability to collect undisturbed, natural-state data (Davis et al., 1992).

Wheat et al. (2010) deployed injection and sampling systems in a CORK on the eastern flank of the Juan de Fuca Ridge, but both of these were only single-hole experiments. Although CORKs have been used in previous experiments, the Tracer Transport experiment described in this paper is the first time multiple CORKs were used together as part of a multi-hole network of CORK sampling points in the subseafloor basement formation. In this multi-hole tracer experiment, the rate of exchange between boreholes is a proxy for net rates of lateral fluid, particle, and solute transport in the area around the borehole (Wheat et al., 2010). The CORKs have been installed, the tracers were injected between 05:13h and 05:19h on August 27, 2010, and the preliminary results from this tracer transport experiment are discussed in this paper. The samples collected by these CORKs are expected to provide a great amount of data that will help in quantifying the microbiological, geochemical, geophysical, and hydrogeological processes and properties within the upper oceanic crust (IODP, 2001).

Several CORKs have been installed in boreholes on the flanks of the Juan de Fuca ridge (see Figure 1). These CORKs are in various locations as well as accessing different

depths within the crust.  This provides the ability to collect data from four dimensions:
latitude, longitude, depth and time.
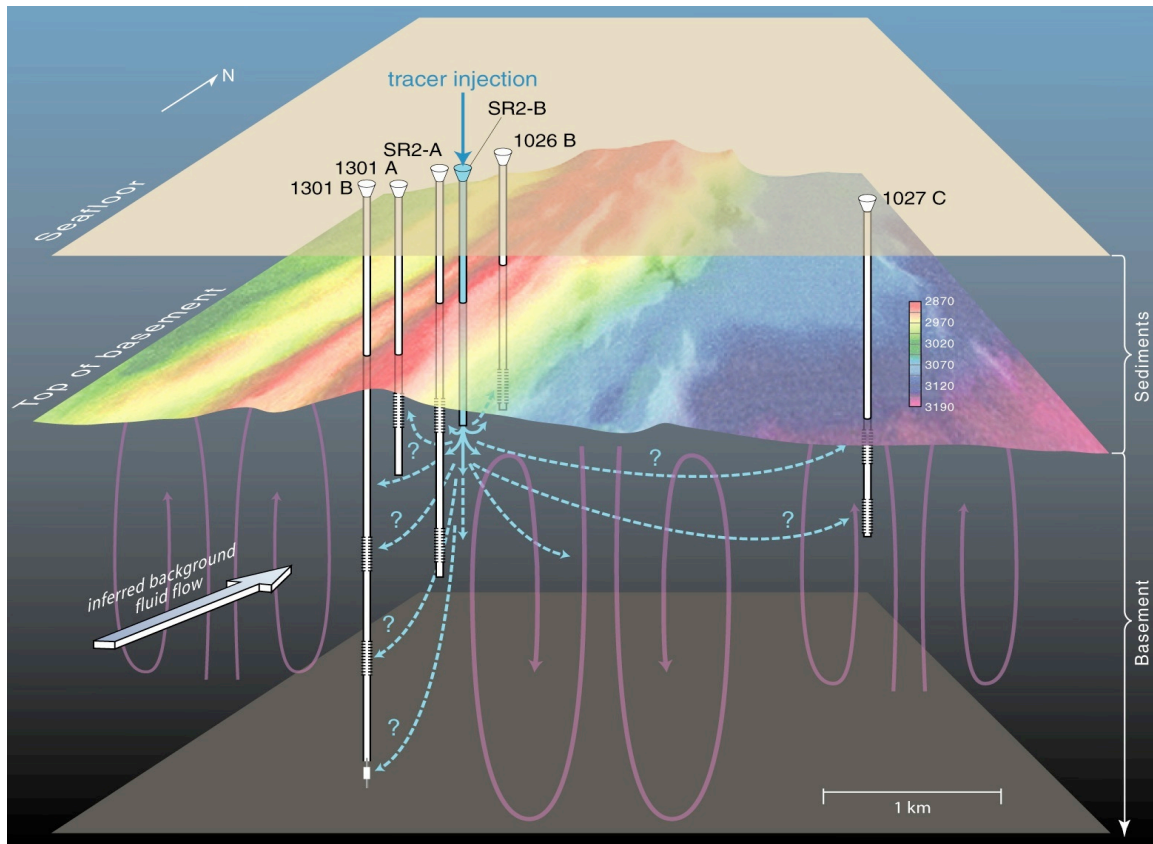


*Figure 1: Cartoon illustrating 3D network of borehole on the eastern flank of the Juan de Fuca Ridge (Fisher et al., 2011).*

## 1.3 Tracer Transport Experiment

The magnitude of water-rock interaction and degree of mixing in an aquifer is a
function of the effective porosity, which is the "fraction of open space involved in fluid
flow", permeability and the hydrodynamic dispersivity, which is the "spreading of solutes
by mechanical dispersion and diffusion" (Cowen, 2004).  Although these properties are
yet to be quantitatively analyzed in an oceanic setting, understanding them is essential to
the accurate modeling of particle transport and deciphering the age distribution of fluids
in the crustal aquifer.  The quantification of these two properties requires direct testing

because their magnitudes vary from site to site (Schulze-Makuch, 2005; Novakowski, 1992).

The tracers that were used in this experiment are fluorescence microspheres, surface-water bacteria that had been fluorescently stained, dissolved gases and dissolved rare earth elements. These tracers were chosen because none of them are harmful to the environment, they can be mixed into injection fluid without difficulty, and they can be easily detected at very low concentrations. Fluorescence microspheres are naturally absent in seawater, and while the other types of tracers are naturally present in seawater, they only exist in extremely low concentrations (Cowen, 2004).

The conceptual basis for a hydrologic tracer injection experiment can be explained rather simply. Injection fluid with a high concentration of detectable tracers is slowly pumped into the ocean basement at an up-gradient injection site, where $C_{in}$ is the tracer concentration of the injectate, and $C_{out}$ is the tracer concentration detected at the monitoring sites (see Figure 2). With simultaneously occurring tracer mixing and spreading, the aquifer fluid flows toward a downstream monitoring site. If the aquifer has complex and heterogeneous flow paths, exchange between several flow networks is possible (Fisher et al., 2011). If the duration of injection is short relative to the measurement period, a dense plume of tracers forms, and will travel through the aquifer, carried by the flow of basement fluid (see Figure 3). Over time, this plume will spread out, increase in volume, and decrease in concentration. Detection of tracers at one or more downstream locations can be used to generate a "breakthrough curve," which is a record of tracer concentration vs. time (see Figure 4). The tracers' arrival time, concentration, and the shape of the breakthrough curve offer insight into the aquifer's

physical (and possibly chemical and biological) processes. Theoretically, if lateral spreading and mixing did not occur throughout the aquifer and the monitoring sites were in a perfectly down-gradient location from the injection site, all of the tracers would be accounted for in the breakthrough curve. In practice, this is nearly impossible. Flow paths tend to be highly complex, and many tracers exhibit non-conservative behavior. This can result in a breakthrough curve with many peaks in tracer concentration at various times (Fisher et al., 2011).
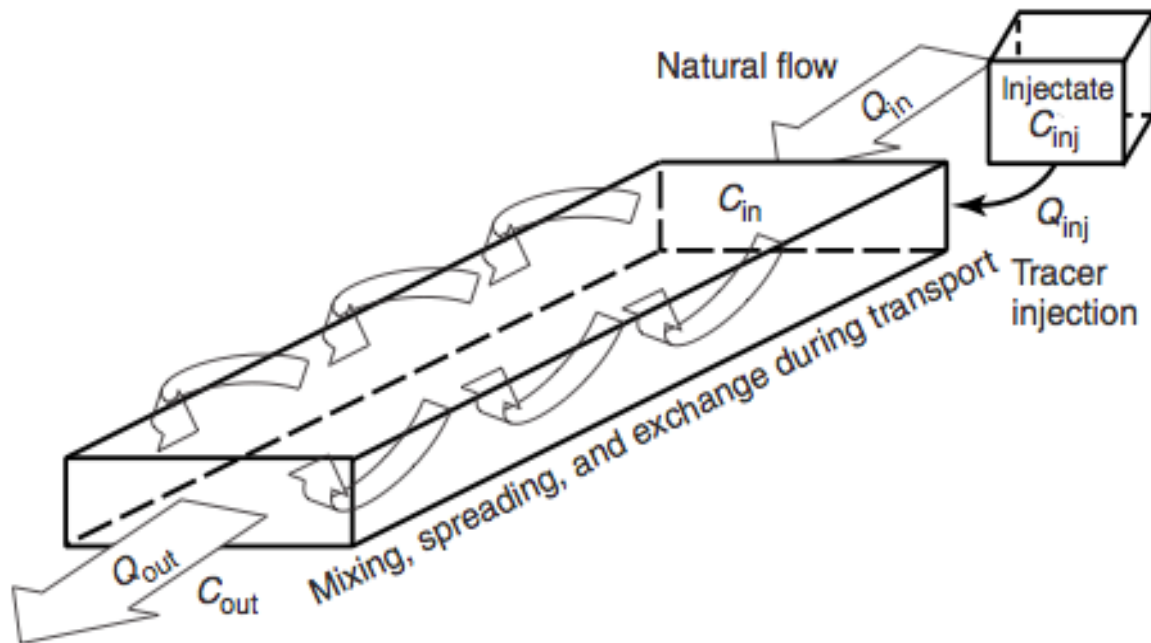


*Figure 2: Natural flow system in which water moves laterally through a rock mass at a constant mass rate, $Q_{in} = Q_{out}$. Injectate is introduced at the upstream end of this system at a constant rate, $Q_{inj}$, for a finite time. Tracer and natural formation fluid are transported downstream, with tracer mixing, spreading, and exchanging with surrounding formation (Fisher et al., 2011).*
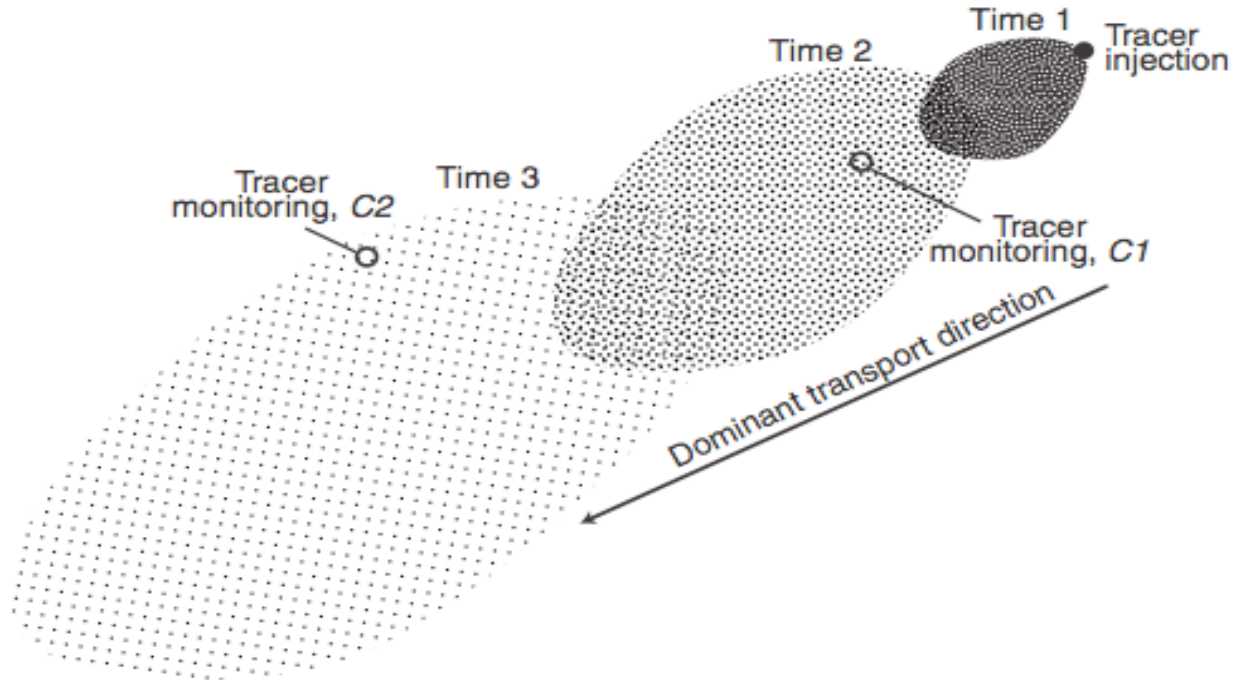
*Figure 3: The tracer is injected for a finite time, leading to the formation of a plume. The plume spreads out, decreases in concentration, and is transported downstream over time. If the tracer is conservative, the mass in the plume will remain constant (Fisher et al., 2011).*
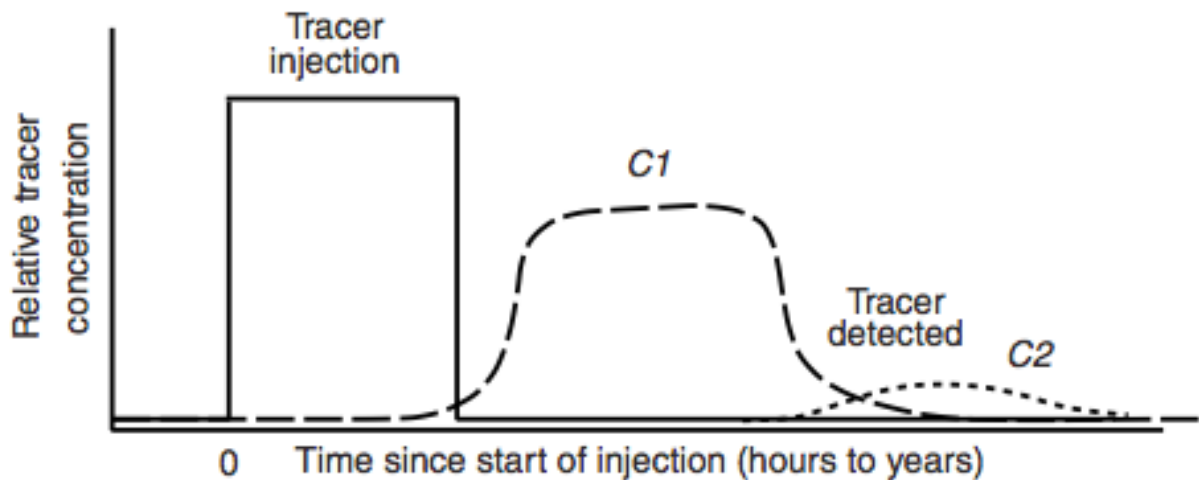


*Figure 4: Schematic chemographs of tracer concentration (breakthrough curves). At the up-gradient end, the period of constant tracer injection is represented with a square wave (solid line). At one or more down-gradient locations (monitoring sites), the chemograph is attenuated, and the center of mass arrives at a time determined by the mean rate of transport (dashed line). The magnitude of the peak concentration is determined by the rate of dilution with unlabeled formation fluid. Farther downstream, the chemograph will arrive later and be more strongly attenuated (dotted line). There can also be a chemograph at a single location that has multiple peaks if there are distinct fluid and tracer transport pathways through the formation (Fisher et al., 2011).*

Through the use of the multi-hole tracer experiment described here, it is possible to determine whether two CORKs are hydrologically connected. This tracer transport experiment is also expected to determine (1) which levels of the crust are hydrologically connected, (2) the magnitude of their connectivity, and (3) the rates and properties of the formation flows (Wheat et al., 2003; Fisher et al., 2005; Altman et al., 2002; Novakowski et al., 1998). Simply detecting the arrival of a tracer particle at a down-stream CORK collection site on the lateral scale of meters to kilometers from the up-stream tracer injection site would be a substantial achievement, but using certain modeling techniques, it will also be possible to interpret this data as needed (Becker and Shapiro, 2000). In the future, scientific experiments that study tracer activity in the ocean basement will be able to take advantage of this three-dimensional network of subseafloor CORK observatories that has been established through the Tracer Transport Project. Determining the most effective way to perform tracer tests on a ridge flank will provide the knowledge necessary to carry out similar experiments in active seafloor spreading areas (Cowen, 2004).

**1.4 Fluorescence Microspheres**

This thesis focuses mainly on the use of fluorescently stained microspheres as tracers (see Figure 5). Although they have been used to study the hydrology of highly complex continental and island groundwater aquifers and to acquire information about the subsurface transport of pathogens and contaminants (Harvey, 1997), this is the first time microspheres have been used in an ocean basement setting.

The microspheres used in this experiment are synthetically manufactured spheres composed of polystyrene. Microspheres of different sizes and fluorescence colors were used: (1) bright blue (BB Coumarin stain) with 0.5 μm diameter, (2) bright blue with 1.0 μm diameter and (3) yellow green (YG Fluorescein) with 1.0 μm diameter (refer to Table 1). They are environmentally benign, readily transported to the ship in a highly concentrated microsphere solution, and they are easily mixed into the injection fluid before being pumping into the seafloor. Microspheres are stable over long periods of time, meaning that their exposure to seawater for up to a year does not affect their size, spherical shape or fluorescence. Because of the stability of their fluorescence stain, microspheres are easily identified in filtered fluid samples, even in low concentrations among with substantial particulate matter. They do not occur naturally in seawater so, with the unfortunate exception of laboratory contamination, a microsphere found in an environmental sample must have come from this subseafloor experiment.

*Table 1: Characteristics of the three types of microspheres used as tracers in this experiment.*

| Characteristic | Microsphere 1 | Microsphere 2 | Microsphere 3 |
|---|---|---|---|
| Diameter (μm) | $1.08 \pm 0.02$ | $1.00 \pm 0.03$ | $0.49 \pm 0.02$ |
| Suspension volume (mL) | 500 | 100 | 100 |
| Dye Compound | YG (Fluorescein) | BB (Coumarin) | BB (Coumarin) |
| Excitation maximum (nm) | 441 | 360 | 360 |
| Excitation minimum (nm) | 486 | 407 | 407 |
| Surface Charge | No charge | Negative | No charge |
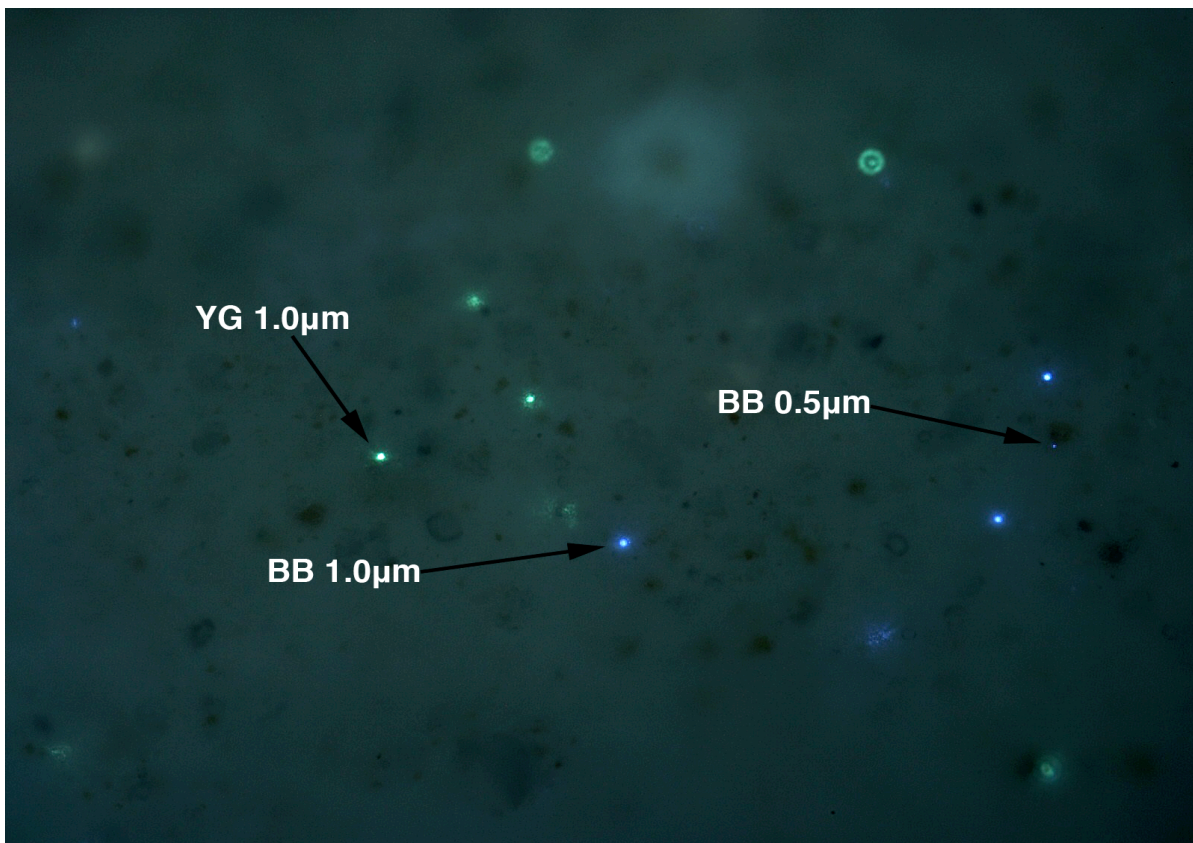
*Figure 5: Color image taken under epifluorescence microscope of microspheres on a black polycarbonate filter under 400x magnification.*

## CHAPTER II
## METHODOLOGY

**2.0 Drilling Ship Methods**

**2.0.0 – Preparation of Tracer Injectate**

Synthetic microspheres were only one type of tracer used as tracers in this experiment, but they are the tracers on which this paper focuses. Prior to injection into the ocean basement, a highly concentrated microsphere solution must be prepared. This concentrated microsphere solution was composed of 700mL of seawater with $4.5 \times 10^{12}$ 1.0 μm YG microspheres, $2.3 \times 10^{13}$ 0.5 μm microspheres, and $3.6 \times 10^{13}$ 1.0 μm YG microspheres. A large cement mixing system below deck of the ship was used to mix the microspheres with water for injection. Microspheres have a density of ~1000 kg/m$^3$, which is slightly lower than the density of seawater (Fisher et al., 2011). This gives the microspheres a neutral to very slightly positive buoyancy, which allows them to maintain their suspension throughout the mixing and transport stages.

**2.0.1 – Injection of Tracer Injectate Fluid**

The microspheres were initially diluted in deionized water (DIW), and prior to injection, they were mixed with freshwater in the cement mixing system (see Figure 6). They were mixed in freshwater in order to minimize microsphere clumping in suspension. The concentration of the microsphere solution that was pumped into the ocean basement formation was $3.5 \times 10^7$ 1.0 μm YG microspheres per liter, $1.9 \times 10^8$ 0.5 μm microspheres per liter, and $2.6 \times 10^8$ 1.0 μm YG microspheres per liter. (Fisher et al., 2011).
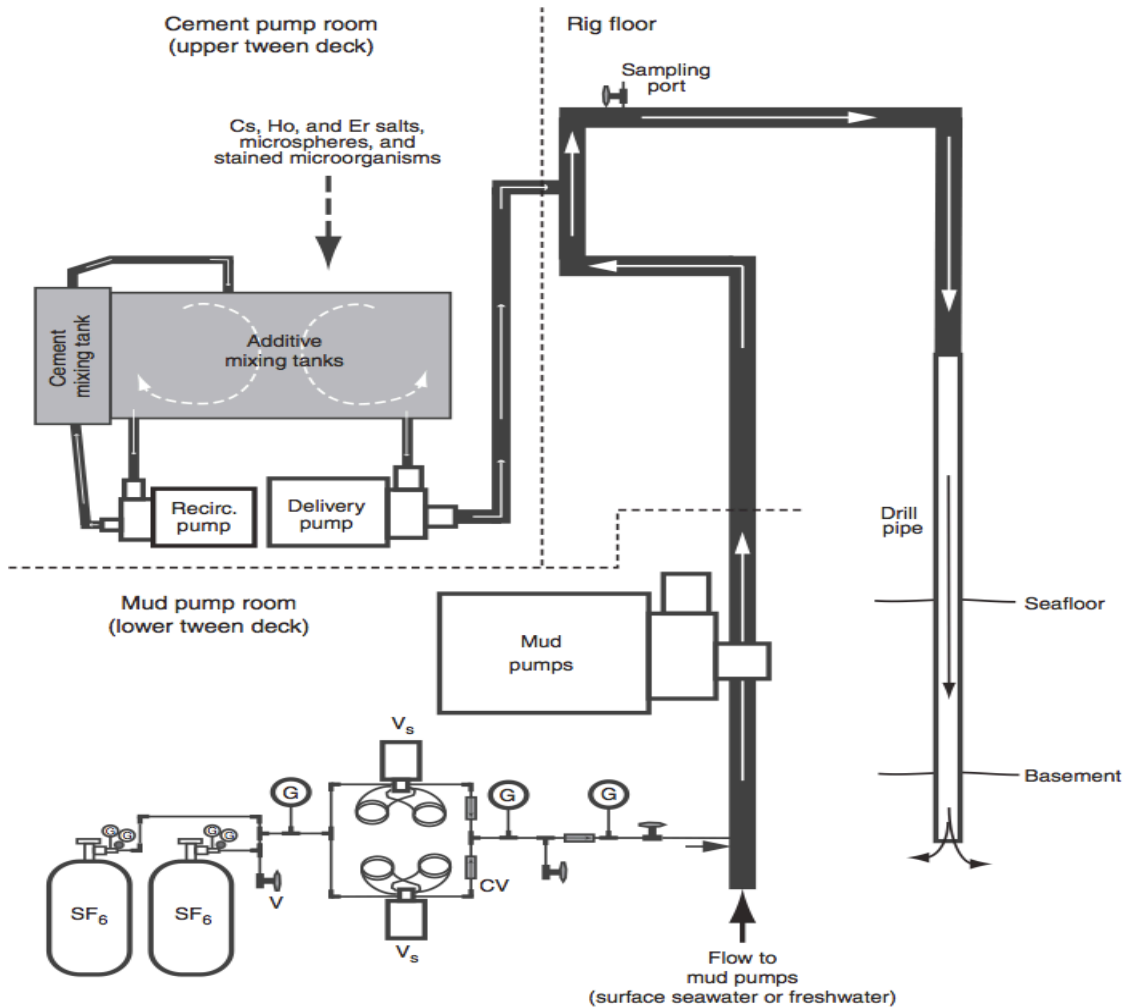
*Figure 6: Schematic of shipboard tracer injection system illustrating pumps, manifolds, mixing points, and rig floor sampling location (not to scale). Mud pumps were used to inject fluid into the formation during the 24 h pumping experiment. Fluid exiting the mud pumps was directed to the rig floor, where it entered the drill pipe. For several brief periods, additional tracers were added to this flow using the cement pump system. Seawater or freshwater was mixed with solutions containing fluorescence microspheres and then added to the flow generated with the mud pump system. A sample port installed on the rig floor allowed the collection of injectate samples (for later analysis) before they were pumped into the drill pipe (Fisher et al., 2011).*

## 2.0.2 – Sampling of Tracer Injectate

Despite knowing the quantities of microspheres added to the solution beforehand, further samples were collected to confirm the microsphere concentration in the injection fluid. Samples were collected as the injectate passed across the rig floor. These samples are essential in determining the extent and variability of possible mixing between the

fluid pumps and the rig floor.  These samples are also important because it was uncertain whether there would be unforeseen difficulties associated with system leaks or maintaining steady rates of flow.

**2.1 Seafloor (CORK) Sample Collection Methods**

**2.1.0 – Sampling and In Situ Filtration**

The GeoMICROBE instrumented sled (see Figure 7), which is an autonomous time series fluid sampling system, is capable of connecting to a CORK observatory (refer to Figure 8 for CORK schematic) in order to collect fluid samples.  The GeoMICROBE system is connected to a fluid delivery lines associated with the CORK in order to draw large volumes of crustal aquifer fluid from the basement to the seafloor.  These extracted fluids pass multiple sensors as well as an in situ filtration and collection system (Cowen et al., 2011).  The GeoMICROBE system has the ability to carry out in-situ filtrations of fluids extracted from the subseafloor basement, and it is also capable of collecting whole fluid samples of up to ~500 mL for manual filtration at a later time.
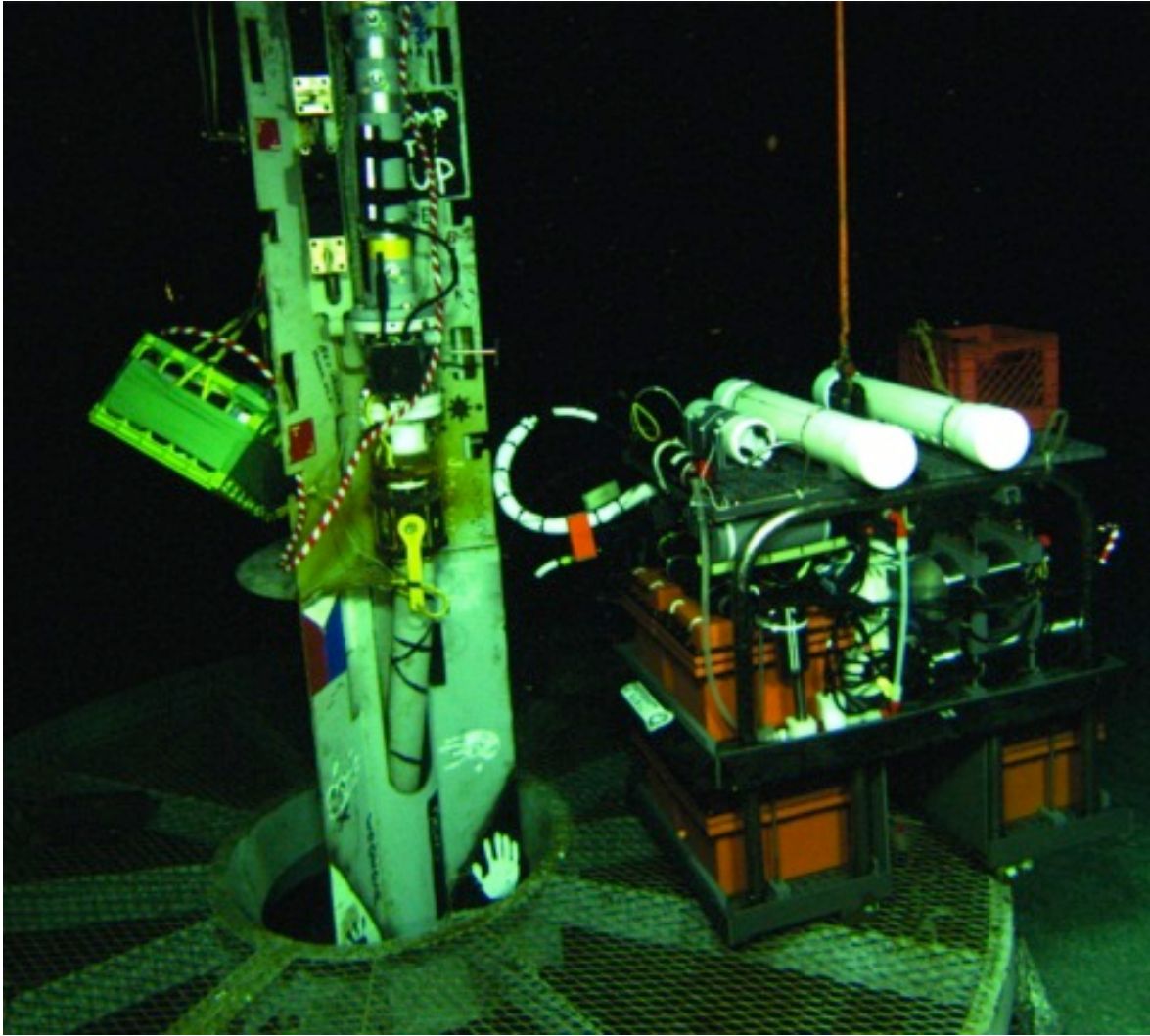
*Figure 7: GeoMICROBE instrumented sled connecting to CORK observatory in borehole (Cowen et al., 2012).*
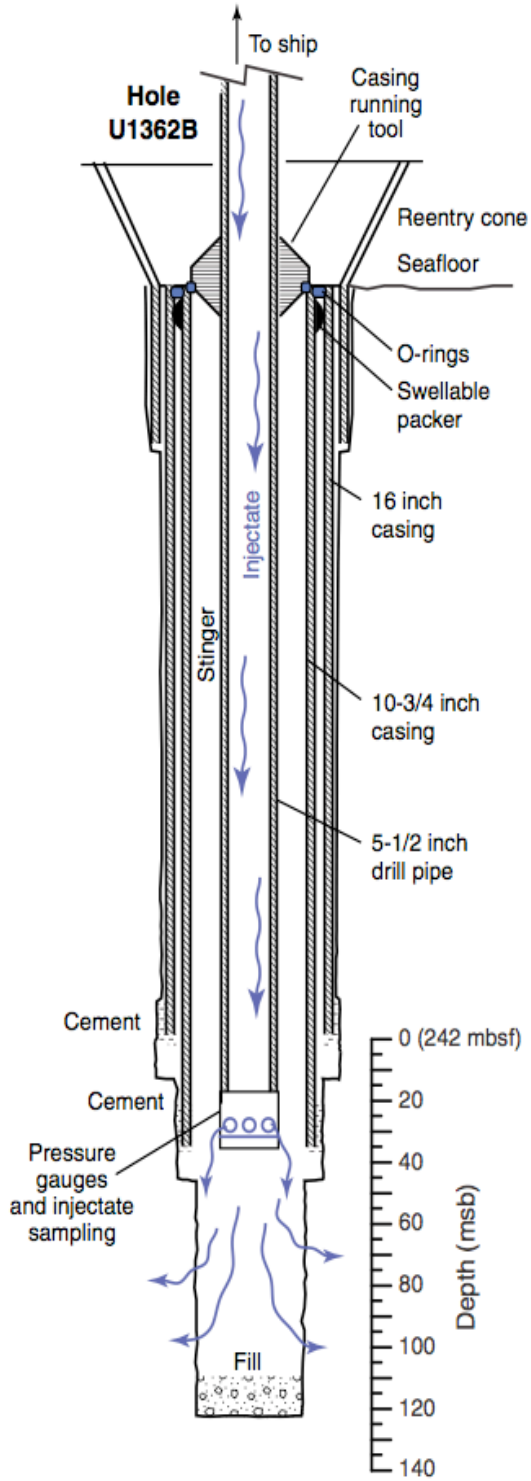
*Figure 8: Schematic diagram of tracer injection geometry inside CORK (Fisher et al., 2011).*

## 2.2 Laboratory Methods

## 2.2.0 – Filtration

## 2.2.0a – Measuring Diameter of Filtration Towers

In order to determine the concentration of microspheres in a sample fluid (microspheres per liter), certain information must be known: the number of microspheres present on the filter and the volume of fluid that passed through the filter. If the microspheres are sparsely distributed on the filter, scanning the entire filter can provide an accurate count of the total number of microspheres present on the filter. If the microspheres are so numerous that counting every microsphere on the filter would be unreasonably tedious, the number of microspheres on a fraction of the filter are counted and used to estimate how many microspheres are on the entire filter. In this case, it would be necessary to know the filtration area in order to compare the area of the scanned region of the filter to the area of the entire filter. Because the filters used in this experiment are circular, the only measurement required to determine the area is the filter radius (or diameter divided by two). There are several ways to measure the diameter of a filtration tower. Two different methods were used for this experiment.

The first method is called the "direct method." The direct method involves measuring the inner diameter of the bottom opening of the tower directly with digital calipers. The inside diameter of the bottom opening of the filtration tower should be the exact same size as the area of the filter through which fluid passes, because the filter is clamped to the bottom of the tower during the filtration process. Because the caliper jaws are parallel, if both jaws are tangential to the circular opening of the tower, the caliper would provide an accurate measurement of the tower diameter. These measurements

17

were carried out three times for each filtration tower, and then the average diameters were calculated for each tower.

Another method used to measure the diameter of a filtration tower is known as the "stain method." For the stain method, deionized water and ferric chloride were combined to make an iron oxide solution. This solution has a rust-colored precipitate that can be captured on filters with 1.0 μm pores. A diluted iron oxide solution composed of several mL of deionized water and ~420μL of iron oxide was vacuum filtered through a white polycarbonate membrane filter with 1.0μm pores. Using digital calipers, the diameter of the circular stain on the filter was carefully measured (see Figure 9). This procedure was repeated three times for each filtration tower and then the average diameter for each tower was calculated. After finding the average measurements for each filtration tower diameter based on two different methods, a comparison of the averages was necessary to determine which method was more reliable. The ultimate goal of this comparison was to arrive at the most reliable measurement of diameter as possible. Because the averages vary between the two methods but do not show a one-sided bias (e.g. one method always provides a larger/smaller measurement), the methods had to be compared as a whole instead of comparing each individual trial. To do this, the standard deviation was calculated, and a statistical t-test was performed with a 95% confidence level (refer to Appendix A for statistical t-test procedure).

*Figure 9: Digital calipers and filters stained with iron oxide solution (photo: Guss)*

## 2.2.0b – Engraving and Cleaning Filtration Towers

Once an accurate measurement of diameter has been obtained for each of the

filtration towers, the diameters and their uncertainties must be engraved on the towers.

After the engraving is completed, it is time to clean the towers as well as possible to

minimize the possibility of contamination. The most thorough cleaning process in this

lab is combustion. To prepare the filtration towers and their bases for combustion, they

must first be soaked in soapy water (1% soap solution) for about 15-20 minutes and then

rinsed with deionized water. Then, the towers and bases are placed in the acid bath for

several days. Upon removal from the acid bath, rinse the towers and bases with

deionized water once more, then combust them.

## 2.2.0c – Test for Microsphere Solubility in Acetone

In order to minimize the possibility of inter-sample contamination of environmental samples in the lab, it was necessary to find a way to destroy the microspheres and clean the equipment in between sample filtration operations. Polysciences Incorporated (the makers of the synthetic microspheres used in this experiment) claimed that acetone is capable of dissolving microspheres. To test the validity of this statement, two drops of known microsphere solution were pipetted onto two improvised* depression slides (one with 1.0 μm YG and one with 0.5μm BB) and left them overnight to dry, which would ensure the immobility of the microspheres. Once dry, the depression slides were covered with cover slips, and the microspheres' presence was verified with the epifluorescence microscope (under 400x magnification). Doing everything with excess caution to avoid contamination, the cover slips were removed and a few drops of acetone were pipetted into each depression. After the acetone had completely evaporated, new cover slips were put onto the depression slides. Each slide was examined again to see if the microspheres had been dissolved. Results from this test indicates that acetone does indeed destroy microspheres; there were no microspheres left on the slides after the introduction of acetone.

*Note: Because no depression slides were available at the time, a volume "holding pen" was made by spreading two-part epoxy around in a circle on a normal glass slide. This was able to retain the microsphere solution as well as the acetone. The epoxy boundary must be high enough so that the coverslip does not touch the microspheres inside the "holding pen."

## 2.2.0d – Filtering Microspheres from Sample Fluids

Filtration of sample fluid potentially containing microspheres followed the procedure described here. The vacuum filtration station was set up with all necessary items laid out: filters, filtration towers, filtration base, slides, cover slips, forceps, acetone, pipettor, pipette tips, disposable pipettes, gloves, DI water, acetone, adhesive sealant (see Figure 10). The filtration tower, filtration base, and forceps were all thoroughly rinsed with acetone, and then rinsed with DI water. New gloves were used for each new sample. A drop or two of DI water was pipetted onto the top of filtration base (this wets the filter and helps it to stick to the base when it is laid down so it will not slide around). Using clean forceps (washed with acetone and DI water as described above), the filter was placed on top of the moistened filtration base. The sample was poured from the bottle into the tower until the tower was about ¾ full, then the manifold valve was opend and sample filtering begun. It is best to pour the remainder of the sample in a manner that keeps the filtration tower between ½ - ¾ full throughout the duration of the filtration. After the fluid was finished filtering, the vacuum was run for an additional 10-15 seconds before removing the filter. With acetone washed forceps, the filter was carefully removed and centered on a pre-labeled microscope slide. A thin, continuous border of water-based EcoGlue® was applied around the filter (roughly the size of a cover slip). A cover slip was placed on top of filter so the glue touches the borders of cover slip, forming a complete seal. The glue must form a completely sealed border around all edges of the cover slip in order to prevent any filtered microspheres from becoming airborne or somehow contaminating the workspace or other samples. Another large slide was placed on top of cover slip and firmly pressed with fingers for

about 15-20 seconds (press firmly and distribute pressure evenly to avoid wrinkles in the

filter or cracks in the cover slip). The filtration tower, filtration base, and forceps were

thoroughly rinsed in acetone. These steps were repeated between each sample filtration

and blank filtration. A blank was collected before each sample filtration. These will be

scanned later to determine the possibility of contamination. For blank filtrations, the

same procedure was used as described above, but used 20-30 mL of DI water instead of

sample fluid. Do not acetone wash the tower, forceps or base between blank and sample

filtrations.

*Note: When filtering any samples that may possibly contain microspheres, remember to change gloves between each step. This may seem excessive, but avoiding contamination and obtaining high-confidence data are the top priorities. When removing the old gloves, peel from the wrist cuff so the glove ends up being inside out. This reduces the chances of microspheres becoming airborne and contaminating the workspace or other samples.*
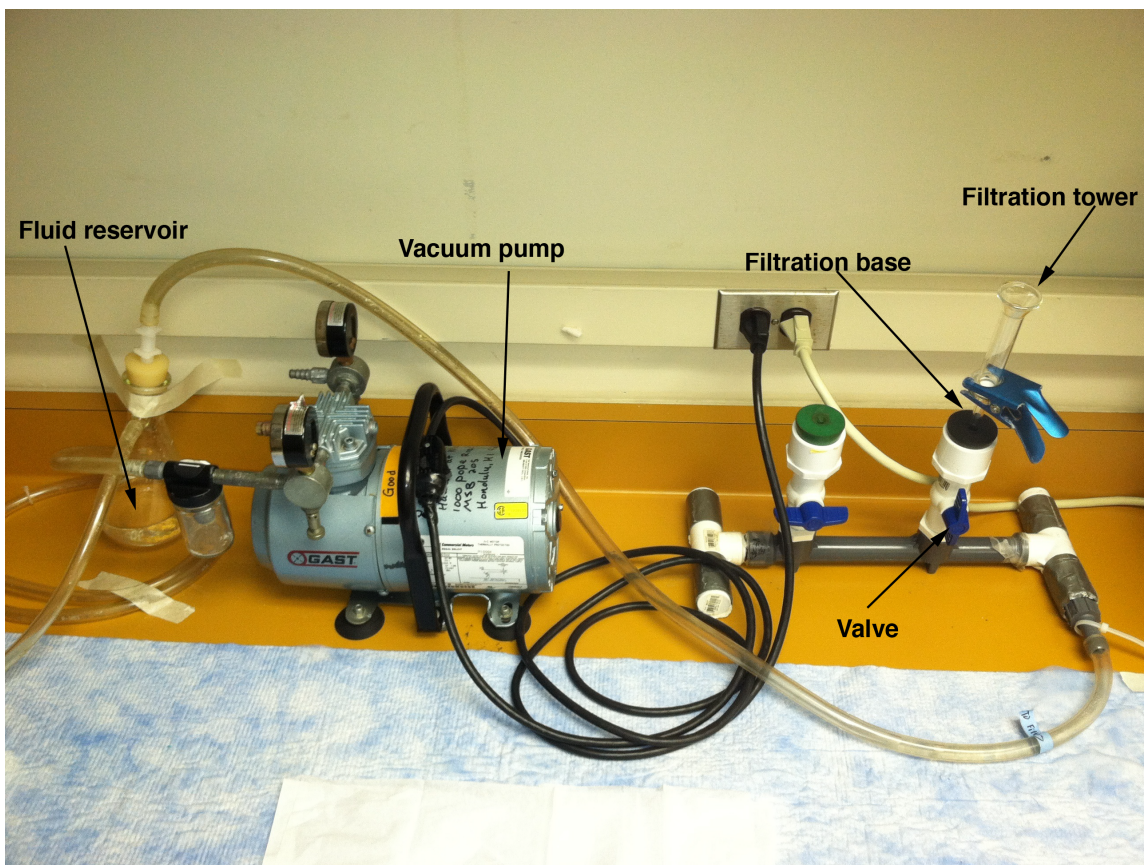


*Figure 10: Vacuum filtration setup with all components assembled correctly.*

## 2.2.0e – Determining Injectate Concentration

It is important to know the concentration of microspheres in the solution that was injected into the ocean basement. This solution is called the injectate, or injection fluid. To determine the concentration of the injection fluid samples (as described in section 2.0.2), the fluid was run through the vacuum filtration process. Once the injection fluid samples were filtered, the number of microspheres on each filter was counted using an epifluorescence microscope (Nikon Eclipse 400). For filters with low microsphere concentrations, the entire filter was scanned, and all of the microspheres were counted. By dividing that number by the milliliters of fluid filtered, the microsphere concentration was obtained (microspheres/mL). For filters with high microsphere concentrations (so high that counting every microsphere on the entire filter was unreasonable), the ocular grid within the right eyepiece of the microscope was utilized. Depending on the concentration of the microspheres on that particular filter, all of the microspheres in either the entire ocular grid or an appropriate subdivision of the grid were counted. In the case of high concentration, selected grid sizes at multiple random locations on the sample were counted until the cumulative counts of microspheres reached approximately 1000, then the average microsphere count per grid was calculated. Because the lengths of the sides of the ocular grid and the lengths of the sides of the subdivisions of the grid are known (see Section 2.2.1a), simple unit conversion is required to extrapolate the data to determine the concentration in microspheres/mL.

Sample Calculation:

$$\frac{10.45 \text{ spheres}}{\text{grid}} \times \frac{1 \text{ grid}}{.0615 \text{ mm}^2 \text{ (grid area)}} \times \frac{209.95 \text{ mm}^2 \text{ (filter area)}}{5 \text{ mL}} = 7{,}135 \text{ microspheres/mL}$$

## 2.2.0f – Determining Effect of 0.4% HCl on Microspheres

Because some of the samples collected throughout this tracer transport experiment would come in contact with hydrochloric acid (some OsmoSampler samples), a solution composed of 0.4% HCl was used to test its effects on the shape, size and fluorescence of the microspheres (see Appendix C).  Appropriate volumes of water and concentrated (12.1 normality) hydrochloric acid needed to create a 100 mL solution of 0.4% HCl were calculated.

Ten drops of 0.5 μm BB microspheres and 10 drops of 1.0 μm YG microspheres were added to the beaker containing 100 mls of 4% HCl solution.  After letting the microspheres remain submerged in hydrochloric acid for just over a month, 2 mL of the acidic solution was vacuum filtered, and the filter was then examined under the epifluorescence microscope.  The microspheres looked the same as they did before the month they spent in the acid.  They remained bright, perfectly round, and easily identifiable.  The 0.4% hydrochloric acid seemed to have no effect on the appearance of the microspheres.


## 2.2.0g – Procedure for "Secondary Rinse" Filtration

Occasionally, fluid samples are stored in the refrigerator for long periods of time before they are filtered.  During this time, it is possible that microspheres can float to the surface (they have a slightly positive buoyancy), become stuck to the inside of the bottle, and not end up on the filter.  Because microspheres are too small to see with the naked eye, something must be done to minimize the possibility of missing a microsphere in this

manner.  What follows is the procedure for what is called a "Secondary Rinse" filtration, which is an attempt to rinse any remaining microspheres from the bottle onto a filter.

Using a clean disposable cup, pour DI water (particle-free fluid) into the container until it is approximately half full.  Put the cap on the container and vigorously shake water in container for 30 seconds.  Set the container down upright, and let is sit for 10 minutes.  Vigorously shake water in container for another 30 seconds.  Set container down upside down, and let it sit for ten more minutes.  Now, carry out the filtration as usual (see section 2.2.0d).

## 2.2.1 – Analysis

### 2.2.1a – UV Microscope Filter Information

The UV filter used when searching for microspheres on the filters is a Nikon "UV-2A Standard UV Cube."  It has an excitation spectrum of 330-380nm, an emission spectrum of 420nm, and a mirror transmission of 400nm.  This filter allows for relatively easy identification of both yellow green (YG) and bright blue (BB) microspheres.

### 2.2.1b – Scanning the Filter

When scanning a filter that potentially holds extremely important microspheres from an environmental sample, it is crucial to be as confident as possible that the entire filter has been scanned.  It is equally important to be confident that the same microsphere has not been counted twice.  The easiest way to assure that these two criteria are met is to start at the topmost edge of the circular filter (12 o'clock) and scan downwards, eventually arriving at the bottommost edge (6 o'clock).  Starting at the top edge of the

filter, use the X-axis stage motion control knob to scan the filter to either the left or the right. Keep scanning until the edge of the filter is reached, and then use the Y-axis stage motion control knob to scan downwards (the filter will move up but the field of view will move down) until the bottom edge of the scanned portion is at the top edge of the field of view. The best way to do this in a way that will minimize the area of the filter that is scanned twice or not scanned at all is to use the edges of the filter. Use the X-axis knob to adjust the filter so that the edge of the filter intersects with 6 o'clock edge of the field of view. Using the Y-axis knob, move downwards on the filter until the edge of the filter that intersected the 6 o'clock edge of the field of view now intersects the 12 o'clock edge of the field of view. By systematically finding a point on the filter and moving it from the exact bottom edge of the field of view to the exact top edge of the field of view, one can almost entirely eliminate the possibility of missing a microsphere or counting the same microsphere twice. Sweep across the filter laterally, moving down one field of view after each sweep, until the bottom of the filter is reached. Remember to use only the X-axis or Y-axis stage motion control knob at a time. By using only one knob at a time, diagonal scanning can be avoided. It is important to avoid this because scanning the filter diagonally greatly decreases the confidence level of scanning of the entire filter, as well as not scanning the same area twice.

# CHAPTER III
# RESULTS

The GeoMICROBE instrumented sled is an autonomous time series sampling system. This autonomous sampling system was used to collect various samples throughout the duration of this tracer transport experiment. The GeoMICROBE sled is capable of connecting to a CORK observatory and (1) collecting up to 500 mL of whole fluids for manual filtration and analysis, and (2) performing in-situ filtrations of 5-10 L of collected fluids. In this section, the analysis of both types of samples are presented: filters resulting from manually filtered whole fluids, and 47 mm in-situ filters returned from the GeoMICROBE sled. The counts of microspheres in the filtered whole fluid samples that were collected from recovery site U1301A can be seen in Table 2. The first appearance of microspheres (of any size or fluorescence stain) was on 10.25.2010 at 03:34h. The small (0.5 μm diameter) BB microspheres were the first to appear in the collection fluid, and only one of them was found. Throughout the remaining whole fluid samples, both sizes of BB microspheres (0.5 μm and 1.0 μm diameter) were found with increasing microspheres per filter increasing time after GeoM deployment (see Figure 12). No YG 1.0 μm diameter microspheres were found in any of these samples.

Subsamples from the whole fluids collected by the GeoMICROBE sled from monitoring site U1301A were filtered again several weeks after the initial filtrations, and these new filters were counted. No microspheres of any size or fluorescence was found on any of these filters (see Table 4).

The in-situ filtrations carried out by the GeoMICROBE sled provided six filters that required analysis. These automated filtrations through 47mm black polycarbonate

membrane filters were done at collection site U1301A. Each of the six filters was manually cut into quarters, resulting in 24 filter quarters. For each filter, three random quarters were scanned. After each quarter was analyzed in its entirety, the numbers of each type of microsphere on the quarters was recorded (see Table 6). Then the three quarter counts for each type of microsphere for each of the filters was averaged (see Table 7). For example, the 0.5μm BB counts for 14.1, 14.3, and 14.4 are (0+2+2)/3 giving an average of 1.33 small BB microspheres per quarter filter of sample 14. For filter 13.2, quite a few (7-10) possible (but not verified) YG microspheres were identified. Although they had the correct color and brightness to be identified as YG microspheres, they are not confirmed because they appeared to be stuck inside the filter or damaged somehow which prevents them from having a definite circular outline. The count for quarter 13.2 was excluded in calculating the average. Therefore, the YG average for filter 13 is (9+2)/2 = 5.5 YG microspheres per quarter filter. Once an average microsphere count had been obtained for each quarter filter, each average was simply multiplied by four to determine the average microsphere count for the entire filter (see Table 8). Dividing the number of a each type of microsphere by the volume of fluid passed through the filter provided the concentration of microspheres in the GeoMICROBE in-situ filtered sample fluid (units = microspheres/L), which can be seen in Table 9. Plotting this data (Figure 18) shows a peak in concentration in YG 1.0 μm microspheres at the initial sample point (July 27 2010), relatively low concentrations on August 27 and November 27, and concentrations of zero at all other points. The BB 1.0 μm microspheres have relatively low concentrations on August 27 and November 27 with a peak concentration on October 27, and have a concentration of zero elsewhere. The BB

28

0.5 µm microspheres have an initial concentration (July 27 2010) of >1 microsphere/L and decline to a concentration of zero by September 27 before returning to just below 1 microsphere/L by December 27.  This data shows that the timing of the peak in concentration varies among the three different types of microspheres.

The in-situ filters obtained by the GeoMICROBE sled were also recounted several weeks after the initial examination, and this secondary analysis revealed that no microspheres of any size or fluorescence were present on the filters (see Table 10).  Once again, this causes the data from the first analysis to be questioned.

Sample fluids were collected at the injection site (U1362B) during the injection as well as 11 months after the initial injection.  The initial sample collection time (t=0 months) at the injection site showed concentrations ranging from $10^7$ to $10^8$ microspheres per mL, depending on the type of microsphere.  The sample collection from nearly a year after the initial injection (t=11months) shows a concentration of microsphere of 4-8 microspheres per mL, a decrease of 7 orders of magnitude (see Table 11).

# Concentration of Microspheres in Injection Fluid
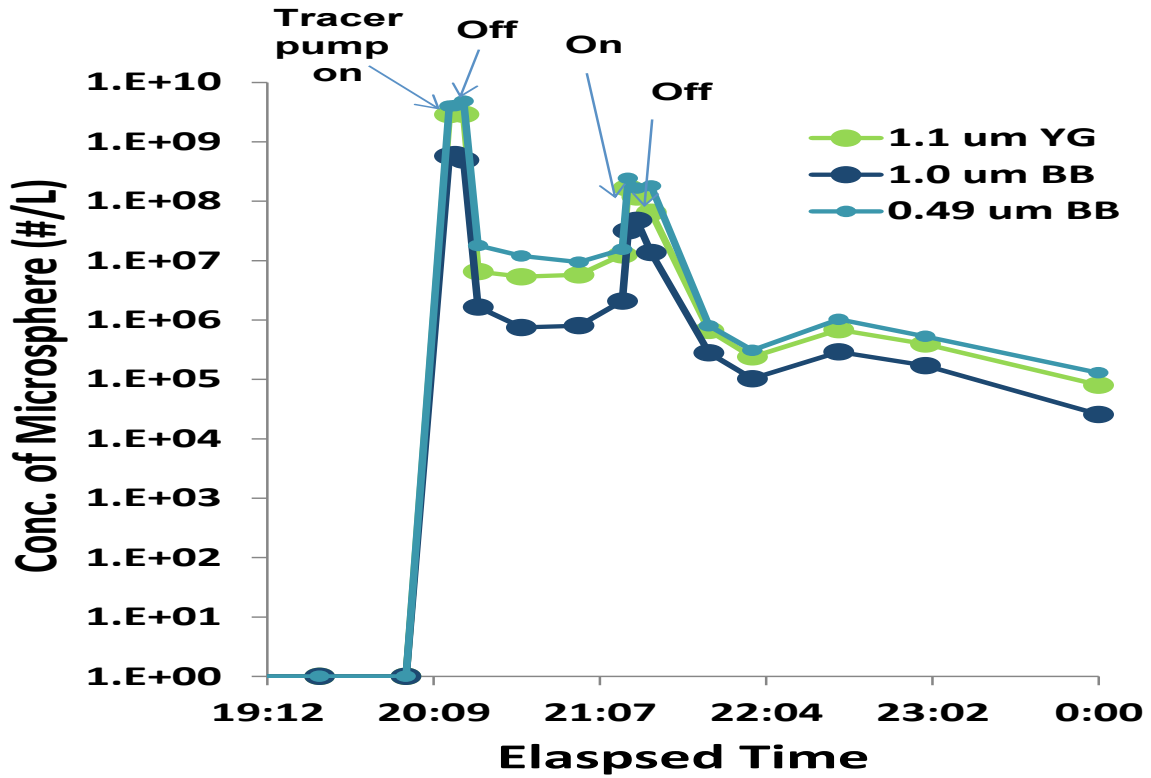


*Figure 11: This plot shows the variation in concentrations of microspheres in the injection fluid that was pumped into hole U1362B (note the y-axis is a log scale). These samples were obtained from a down-hole sampling port near the seafloor. The units on this plot are given in number of microspheres per mL. By integrating the area under the curve, it is possible to obtain the total number of microspheres injected throughout the entire duration of the injection period.*

Table 2: These are the counts of microspheres from the whole fluid GeoMICROBE samples that I filtered in the lab. These samples were collected from hole U1301A. Note: this is preliminary data; the fluids were filtered again and recounted.

| Collection Time | Sample # | Volume (mL) | YG 1.0µm | BB 1.0µm | BB 0.5µm |
|---|---|---|---|---|---|
| 7.27.2010 (03:56) | 1 | 125 | 0 | 0 | 0 |
| 8.26.2010 (03:49) | 2 | 130 | 0 | 0 | 0 |
| 9.25.2010 (03:46) | 3 | 62 | 0 | 0 | 0 |
| 10.25.2010 (03:34) | 4 | 56 | 0 | 0 | 1 |
| 11.24.2010 (04:05) | 5 | 137 | 0 | 4 | 6 |
| 12.24.2010 (3:41) | 6 | 133 | 0 | 7 | 12 |

*DI blanks were filtered before each of these samples in order to check for contamination. While there were many fluorescence particles on the blank filters, no microsphere was found on any of the blanks. This suggested that the microspheres found on the sample filters were not due to contamination. After further examination, it was determined that the 'non-microsphere' fluorescence particles on the blank filters were present before filtration of fluid; these particles came stock with the polycarbonate membrane filters.*
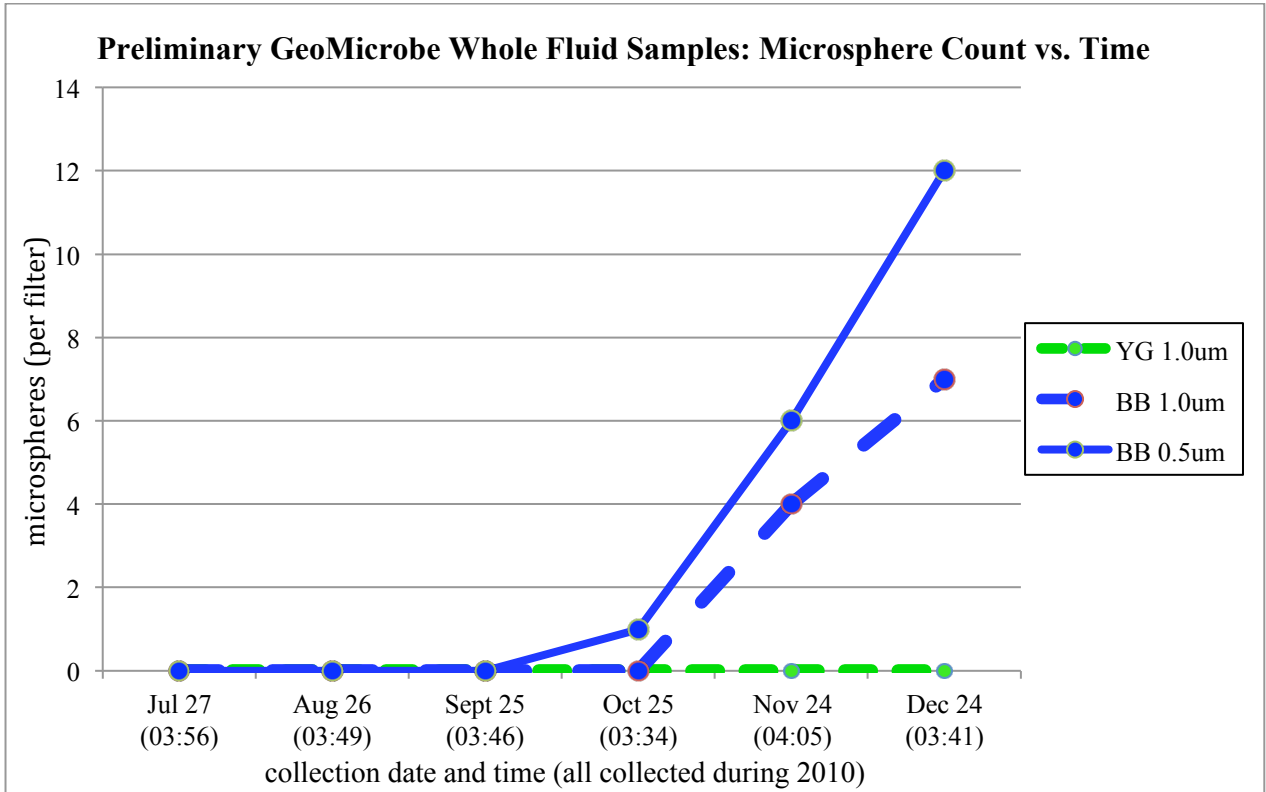
*Figure 12: This plot shows the number of microspheres counted on each GeoMICROBE whole fluid sample filter. These are not the concentrations, simply the numbers of microspheres per filter. Note: this is preliminary data; the fluids were filtered again and recounted.*

Table 3: Concentrations (per mL) of microspheres in the GeoMICROBE whole fluid samples that were filtered in the lab. To get the concentration, I simply divided the number of microspheres by the volume of sample that was passed through the filter. Note: this is preliminary data; the fluids were filtered again and recounted.

| Collection Time | Sample # | Volume (mL) | YG 1.0um | BB 1.0um | BB 0.5um |
|---|---|---|---|---|---|
| 7.27.2010 (03:56) | 1 | 125 | 0 | 0 | 0 |
| 8.26.2010 (03:49) | 2 | 130 | 0 | 0 | 0 |
| 9.25.2010 (03:46) | 3 | 62 | 0 | 0 | 0 |
| 10.25.2010 (03:34) | 4 | 56 | 0 | 0 | 0.018 |
| 11.24.2010 (04:05) | 5 | 137 | 0 | 0.029 | 0.044 |
| 12.24.2010 (03:41) | 6 | 133 | 0 | 0.053 | 0.090 |
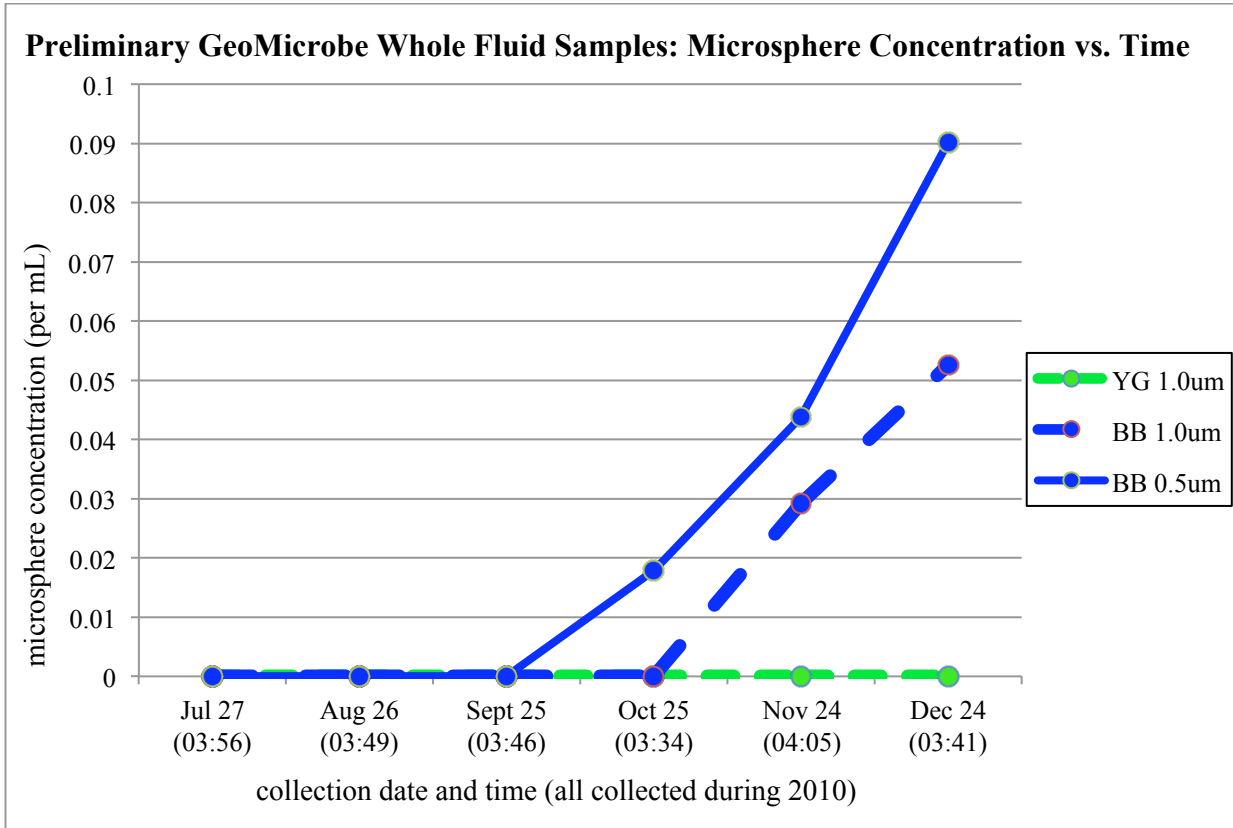
*Figure 13: These are the concentrations of microspheres in the monthly whole fluid samples collected by the GeoMICROBE sled. These concentrations are in units of microspheres/mL. Note: this is preliminary data; the fluids were filtered again and recounted.*

Table 4: Verified counts of microspheres from manually filtered whole fluid collected by the GeoMICROBE at U1301A (microspheres per filter).

| Collection Time | Sample # | YG 1.0µm | BB 1.0µm | BB 0.5µm |
|---|---|---|---|---|
| 7.27.2010 (03:56) | 1 | 0 | 0 | 0 |
| 8.26.2010 (03:49) | 2 | 0 | 0 | 0 |
| 9.25.2010 (03:46) | 3 | 0 | 0 | 0 |
| 10.25.2010 (03:34) | 4 | 0 | 0 | 0 |
| 11.24.2010 (04:05) | 5 | 0 | 0 | 0 |
| 12.24.2010 (3:41) | 6 | 0 | 0 | 0 |
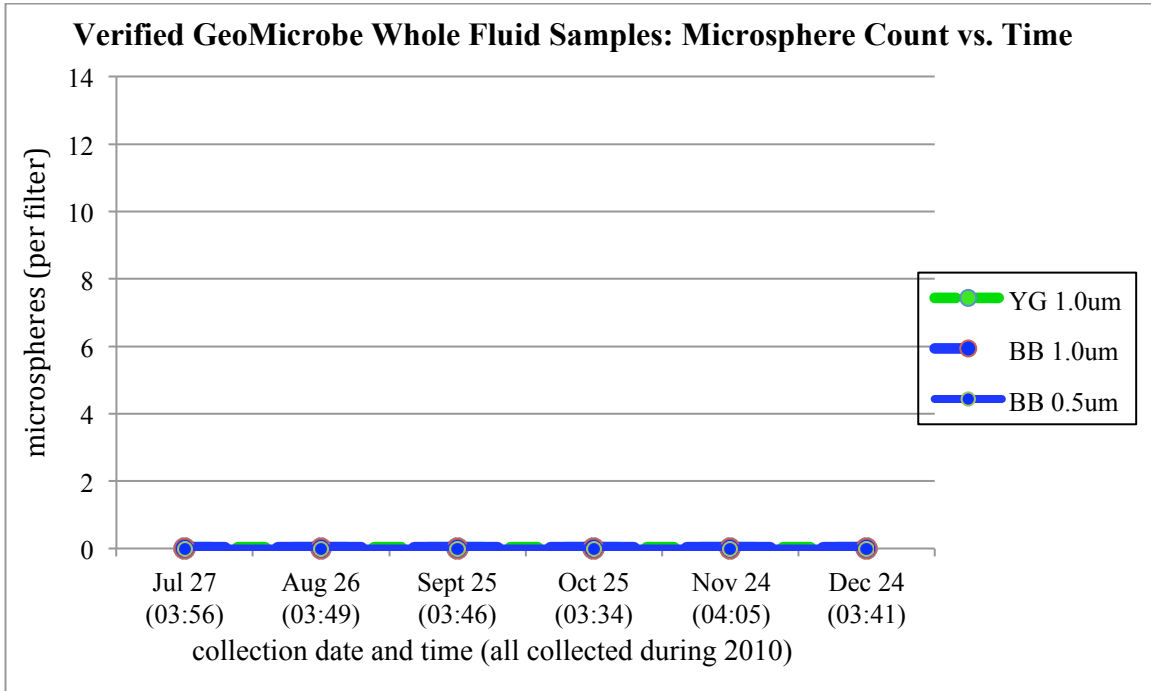
*Figure 14: This is a plot of the microspheres per filter from the re-filtered and re-counted GeoMICROBE whole fluid samples.*

Table 5: More fluid from the whole fluid samples was filtered, and these new filters were counted.  These are the concentrations of microspheres from these filters (microspheres per mL).  These concentrations were determined by dividing the number of microspheres per filter by the volume of fluid that passed through the filter.

| Collection Time | Sample # | YG 1.0um | BB 1.0um | BB 0.5um |
|---|---|---|---|---|
| 7.27.2010 (03:56) | 1 | 0 | 0 | 0 |
| 8.26.2010 (03:49) | 2 | 0 | 0 | 0 |
| 9.25.2010 (03:46) | 3 | 0 | 0 | 0 |
| 10.25.2010 (03:34) | 4 | 0 | 0 | 0 |
| 11.24.2010 (04:05) | 5 | 0 | 0 | 0 |
| 12.24.2010 (03:41) | 6 | 0 | 0 | 0 |
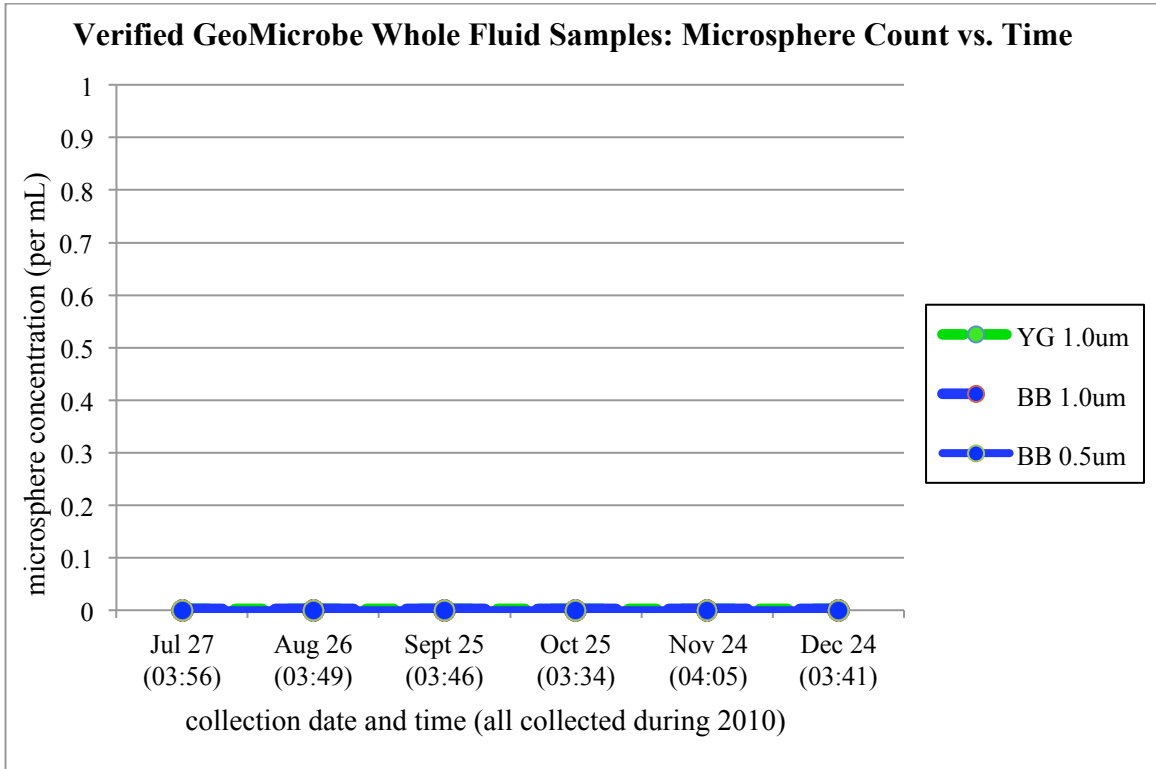
*Figure 15: This is a plot of the concentrations of microspheres from the re-filtered and re-counted GeoMICROBE bag samples (microspheres/mL).*

Table 6: These samples are 47mm in-situ filtration filters collected by the GeoMICROBE sled from hole U1301A.  There were six filters total, numbered 13-18.  Once retrieved, each filter was cut into quarters.  This gave a total of 24 filters that could be counted (13.1, 13.2, 13.3, 13.4, 14.1, etc).  For these counts a random quarter from each filter was scanned in its entirety.  Note: this is preliminary data; the filters were later recounted.

| Collection Date | Sample # | YG 1.0µm | BB 1.0µm | BB 0.5µm |
|---|---|---|---|---|
| 7.27.2010 | 13.2 | possible… | 0 | 0 |
| 7.27.2010 | 13.3 | 9 | 0 | 0 |
| 7.27.2010 | 13.4 | 2 | 0 | 5 |
| 8.27.2010 | 14.1 | 1 | 1 | 0 |
| 8.27.2010 | 14.3 | 0 | 1 | 2 |
| 8.27.2010 | 14.4 | 0 | 0 | 2 |
| 9.27.2010 | 15.1 | 0 | 0 | 0 |
| 9.27.2010 | 15.2 | 0 | 0 | 0 |
| 9.27.2010 | 15.4 | 0 | 0 | 0 |
| 10.27.2010 | 16.1 | 0 | 5 | 0 |
| 10.27.2010 | 16.3 | 0 | 6 | 0 |
| 10.27.2010 | 16.4 | 0 | 0 | 0 |
| 11.27.2010 | 17.1 | 0 | 1 | 0 |
| 11.27.2010 | 17.3 | 1 | 0 | 0 |
| 11.27.2010 | 17.4 | 0 | 0 | 0 |
| 12.27.2010 | 18.1 | 0 | 0 | 0 |
| 12.27.2010 | 18.2 | 0 | 0 | 3 |
| 12.27.2010 | 18.3 | 0 | 0 | 0 |

Table 7: Average number of microspheres counted on the 47mm in-situ quarter filters. These values were found by averaging the counts for the three quarters from each filter that was analyzed. (See note below Graph 6 that addresses the possible YG microspheres found on filter 13.2). Note: this is preliminary data; the filters were later recounted.

| Collection Date | Sample # | YG 1.0µm | BB 1.0µm | BB 0.5µm |
|---|---|---|---|---|
| 7.27.2010 | 13 | 5.5 | 0 | 1.67 |
| 8.27.2010 | 14 | 0.33 | 0.67 | 1.33 |
| 9.27.2010 | 15 | 0 | 0 | 0 |
| 10.27.2010 | 16 | 0 | 3.67 | 0 |
| 11.27.2010 | 17 | 0.33 | 0.33 | 0 |
| 12.27.2010 | 18 | 0 | 0 | 1 |
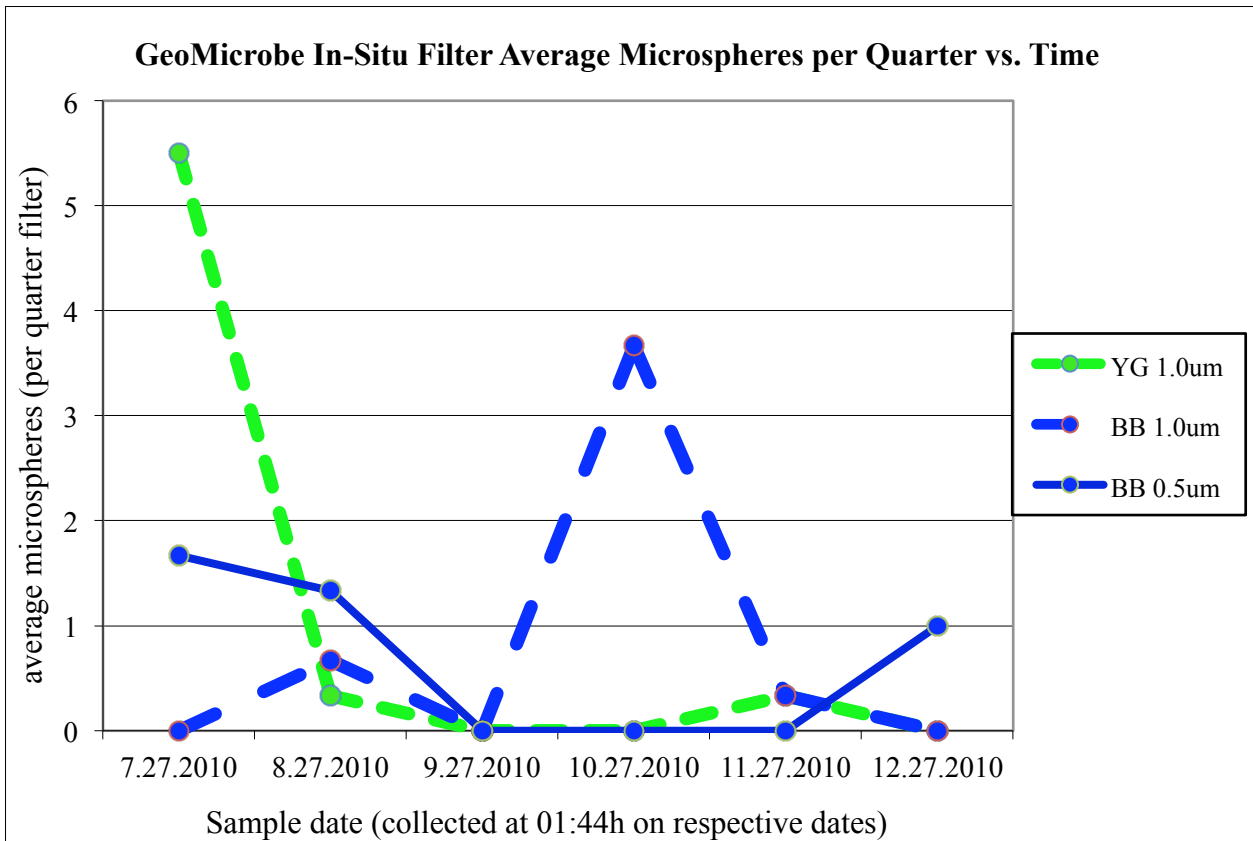
*Figure 16: For this plot, I averaged the microsphere counts for each filter for each type of microsphere. For example, the small BB counts for 13.2\*, 13.3, and 13.4 are (0+0+5)/3 giving and average of 1.67 small BB microspheres per quarter filter of sample 13. Note: this is preliminary data; the filters were later recounted.*

*\*Note: For filter 13.2, I found quite a few (7-10) possible YG microspheres. They are not confirmed because they appear to be stuck inside the filter or damaged somehow which prevents them from having a definite circular outline, but they had the correct color and brightness to be a possible YG microsphere. This number of approximately 8 YG spheres seems to be consistent with the YG counts on the other quarter filters from sample 13. I excluded the count for quarter 13.2 in calculating the average. Therefore, the YG average for filter 13 is (9+2)/2 = 5.5 YG spheres per quarter filter.*

Table 8: These are the numbers of microspheres on the whole 47mm in-situ filters from the GeoMICROBE sled. These values were obtained by multiplying the average counts of the quarter filters (see Table 11) by four to extrapolate the data over the entire filter. Note: this is preliminary data; the filters were later recounted.

| Collection Date | Sample # | YG 1.0µm | BB 1.0µm | BB 0.5µm |
|-----------------|----------|----------|----------|----------|
| 7.27.2010 | 13 | 22 | 0 | 6.68 |
| 8.27.2010 | 14 | 1.32 | 2.68 | 5.32 |
| 9.27.2010 | 15 | 0 | 0 | 0 |
| 10.27.2010 | 16 | 0 | 14.68 | 0 |
| 11.27.2010 | 17 | 1.32 | 1.32 | 0 |
| 12.27.2010 | 18 | 0 | 0 | 4 |
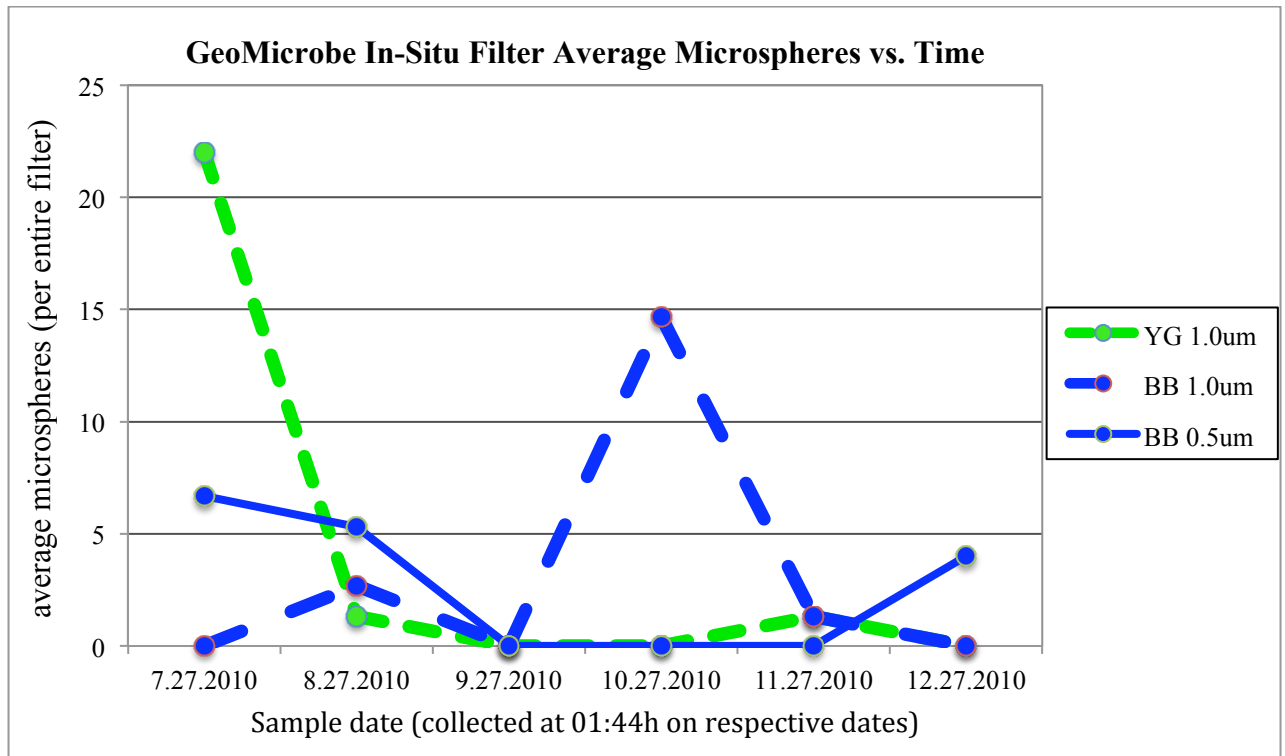


Figure 17: This plot shows the extrapolated average microsphere counts on the entire 47mm GeoMICROBE in-situ filters. Note: this is preliminary data; the filters were later recounted.

Table 9: These are the microsphere concentrations (per mL) for the 47mm GeoMICROBE in-situ filters (in units of microspheres/L). These values were obtained by dividing the number of microspheres on the entire filter by the volume of fluid that passed through the filter. Note: this is preliminary data; the filters were later recounted.

| Collection Date | Sample # | Volume (L) | YG 1.0µm | BB 1.0µm | BB 0.5µm |
|---|---|---|---|---|---|
| 7.27.2010 | 13 | 5.228 | 4.21 | 0 | 1.28 |
| 8.27.2010 | 14 | 5.195 | 0.25 | 0.52 | 1.02 |
| 9.27.2010 | 15 | 5.081 | 0 | 0 | 0 |
| 10.27.2010 | 16 | 5.103 | 0 | 2.88 | 0 |
| 11.27.2010 | 17 | 4.829 | 0.27 | 0.27 | 0 |
| 12.27.2010 | 18 | 4.717 | 0 | 0 | 0.85 |
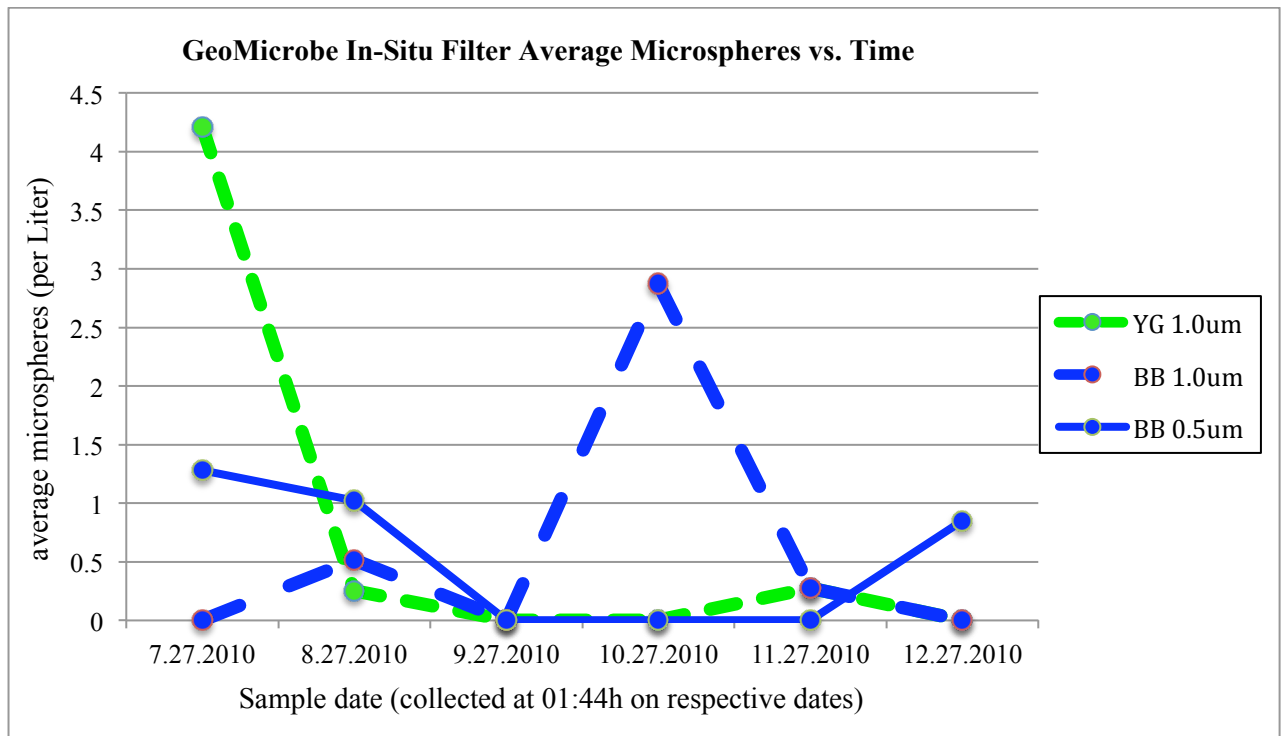


*Figure 18: "Breakthrough curve" for the monthly 47mm in-situ filters. This plot shows the concentration of microspheres in the fluids collected by the GeoMICROBE sled from July-December, 2010. Note: this is preliminary data; the filters were later recounted.*

Table 10: The 47mm GeoMICROBE in-situ filters were recounted several weeks after the initial count, and no microspheres of any size or fluorescence were found on any of the quarters. These are the resulting microsphere concentrations for the in-situ filtrations (in units of microspheres/L).

| Collection Date | Sample # | Volume (L) | YG 1.0µm | BB 1.0µm | BB 0.5µm |
|---|---|---|---|---|---|
| 7.27.2010 | 13 | 5.228 | 0 | 0 | 0 |
| 8.27.2010 | 14 | 5.195 | 0 | 0 | 0 |
| 9.27.2010 | 15 | 5.081 | 0 | 0 | 0 |
| 10.27.2010 | 16 | 5.103 | 0 | 0 | 0 |
| 11.27.2010 | 17 | 4.829 | 0 | 0 | 0 |
| 12.27.2010 | 18 | 4.717 | 0 | 0 | 0 |
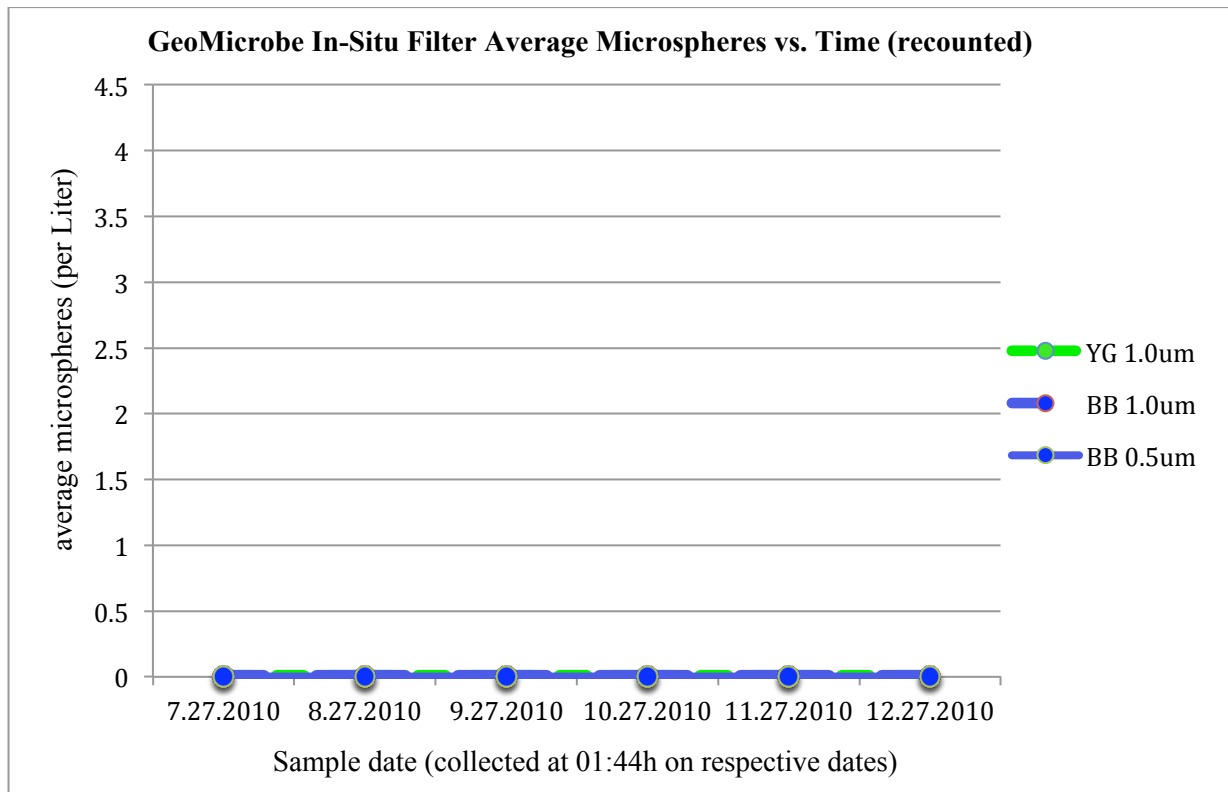


*Figure 19: The 47mm GeoMICROBE in-situ filters were recounted several weeks after the initial count, and no microspheres of any size or fluorescence were found on any of the quarters. These are the resulting microsphere concentrations for the in-situ filtrations (in units of microspheres/L).*

*Table 11: These are the concentrations of each type of microsphere from fluids collected at the injection site (U1362B) at the initial injection time (t=0 months), and a later collection time (t=11 months).*

| Tracer | Conc. @ t = 0 months (spheres/mL) | Conc. @ t = 11 months (spheres/mL) |
|---|---|---|
| YG 1.0 μm | $1.9 \times 10^8$ | 8 |
| BB 1.0 μm | $3.5 \times 10^7$ | 0 |
| BB 0.5 μm | $2.6 \times 10^8$ | 4 |

**CHAPTER IV**
**DISCUSSION**

Although microspheres were initially found associated with samples from collection site U1301A, further analysis showed that the data supporting these preliminary observations may not be reliable. The current revised assessment indicates that no microspheres were found in either the whole fluid GeoMICROBE samples or the in-situ filters obtained by the GeoMICROBE from collection site 1301A over the August, 2010 to February, 2011, time frame. On the other hand, the samples collected from the injection site show a vast decrease in microsphere concentration; the majority of the microspheres injected at U1362B are no longer at the injection site, their concentration having decreased by 7 orders of magnitude within 11 months.

The data gathered in this experiment does not necessarily indicate that the sites of these two CORK observatories (U1362B and U1301A) are not hydrogeologically connected; there are several possible explanations for the absence of microspheres in samples collected from U1301A and U1362A. It is possible that the microspheres may be trapped somewhere in the rock formation near the injection site, such that they are recovered by fluid sampling. This could be explained by the process of gravity settling, which is simply the physical mechanism of particles sinking in fluid due to their negative buoyancy. However, given the extremely high initial concentration, slightly positive buoyancy of the microspheres, and close proximity of sampling to the injection site (the fluid samples were collected at the same cite as the initial microsphere injection site), this explanation is very unlikely. It is possible that the positive buoyancy of the microspheres could cause them to become stuck in overlying pores due to gravity ascension, but the apparent rigorous circulation of basement fluid would likely keep the microspheres in

suspension. The microspheres also may have dissolved in the seawater after injection, but this is not likely because tests were done prior to injection that verified the microspheres' long-term stability in seawater, including at elevated temperatures (to >60°C). Another possibility is that the microspheres are being advectively transported in directions that bypass the collection sites (see Figure 20), too far from the established collection sites to be detected by fluid sampling. Advective transport is the physical process of particle transport within a moving fluid due to the fluid's bulk flow. This is the postulated primary mechanism driving the particle transport addressed in this paper. A plausible alternative explanation, however, is that the microspheres are traveling towards the collection sites, but they just had not yet arrived by December 27, 2010, the latest sampling time analyzed. Another possible explanation for the absence of microspheres in the recovered fluids is that the sample sizes are too small. If the concentration of microspheres in the recovered fluids is extremely low, the volume of sampled and subsequently filtered fluid would need to be increased in order to reach the minimum detection limit of one microsphere per filter. The limitations on increasing the volume of filtered fluid and collected fluids are that the GeoMICROBE sled is only capable of collecting up to 500 mL of whole fluid in one sample. If the volume of the in-situ filtrations was increased much more than 1000 mL, there would likely be too much particulate matter on the filter, making the analysis of sample filters very difficult.

The first set of data was analyzed and thought to contain microspheres. Upon further analysis, the data was found to be questionable. The authenticity of a microsphere can be determined if the UV filter on the microscope was switched from the Nikon UV-2A "Standard UV Cube" with an excitation spectrum of 330-380nm, an emission

spectrum of 420nm, and a mirror transmission of 400nm to the Nikon B-2A "Standard

FITC Cube" with an excitation spectrum of 450-490nm, an emission spectrum of 515nm,

and a mirror transmission of 500nm.  Under the Nikon Standard FITC Cube, YG

microspheres remain yellow-green, and BB microspheres turn bright white, but both are

still perfectly circular and easily identifiable.  If the questionable particle disappears, it is

not a microsphere.  This method of verification made the data obtained from the initial

analyses of GeoMICROBE samples questionable.

The tracer injection site U1362B is located at 47° 45.4997' N, 127° 45.7312' W.

The remote site where the fluid samples were collected and have been analyzed,

U1301A, is located at 47° 45.209' N, 127° 45.833' W.  Assuming a perfectly straight,

lateral path of transport, the distance between these two sites is 0.5535 kilometers, or

553.5 meters.  Because the time of injection is known (between 05:13h and 05:19h on

August 27, 2010), the duration of transport can be calculated when the initial detection

occurs, indicating their arrival time.  The rate of particle transport (for which

microspheres are a proxy) can be calculated by simply dividing the distance (553.5

meters) by the time required for the microspheres to travel between the sites (the time

elapsed between injection time to arrival time).  This rate of transport will be based on

the assumption of a perfectly straight, lateral path of transport, but practice this is highly

unlikely.  Therefore, it is safe to assume that the microspheres will experience some

lateral and vertical deviations from a perfectly straight transport path.  This means that

the calculated rate of transport based on this assumption is a conservative rate (i.e., the

slowest possible transport rate).  Since it is highly likely that the travel distance between

the two sites is greater than the minimal straight line distance, the rate of travel is likely to be greater than the calculated rate.

Despite the probable large range of basement properties, Fisher and Becker (2000) calculated that lateral subseafloor fluid fluxes on a global basis have an estimated range of 0.3 – 30 meters per year for seafloor with ages younger than 20 million years, and the range decreases to 0.03 – 3 meters per year for seafloor ages between 40 and 65 million years. The eastern flank of the Juan de Fuca Ridge where this tracer transport experiment was conducted is composed of 3.5 million year old ocean crust (Fisher et al., 2011). Previous studies (Skagius and Neretnieks, 1986, Birgersson and Neretnieks, 1990) showed that conservative tracers in continental crystalline rock have diffusion rates of approximately $10^{-10}$ – $10^{-9}$ cm per second, or ~0.32 – 3.15 meters per year. These values are close to Fisher and Becker's low estimated transport rates in oceanic basement rock. Based on the calculations made by Fisher and Becker, the injected microspheres could take 16 – 1660 years to be transported from U1362B to U1301A, which is a lateral distance of 500 meters away. Based on these same calculations, the microspheres could have a transport time of approximately 6 – 660 years to travel from injection site U1362B to collection site U1301A. The rates observed in continental crystalline rock indicate that if the physical properties are of this crystalline rock structure is similar to that of the eastern flank of the Juan de Fuca Ridge, microsphere arrival is not yet expected.

If one or more of the dissolved tracers that were pumped into the injection sites are detected in the fluids sampled from the collection sites, this would verify their ability to be transported through the ocean crust. This would indicate that dissolved tracers exhibit different tracer transport behavior than colloidal tracers (ie. microspheres). If

dissolved tracers were detected at an earlier sample date than the microspheres, this would suggest that dissolved tracers are transported through the Juan de Fuca Ridge ocean basement at higher rates than colloidal solids. Dissolved tracers arriving at a collection site before microspheres could provide information of the porosity and interconnectedness of the ocean crust between the injection site and the sampling site. If the pore sizes are large enough to allow dissolved tracers (in water) to travel between sites but not microspheres, the pore diameters in the subseafloor crust in between the sites might be < 0.5 – 1.0 μm.
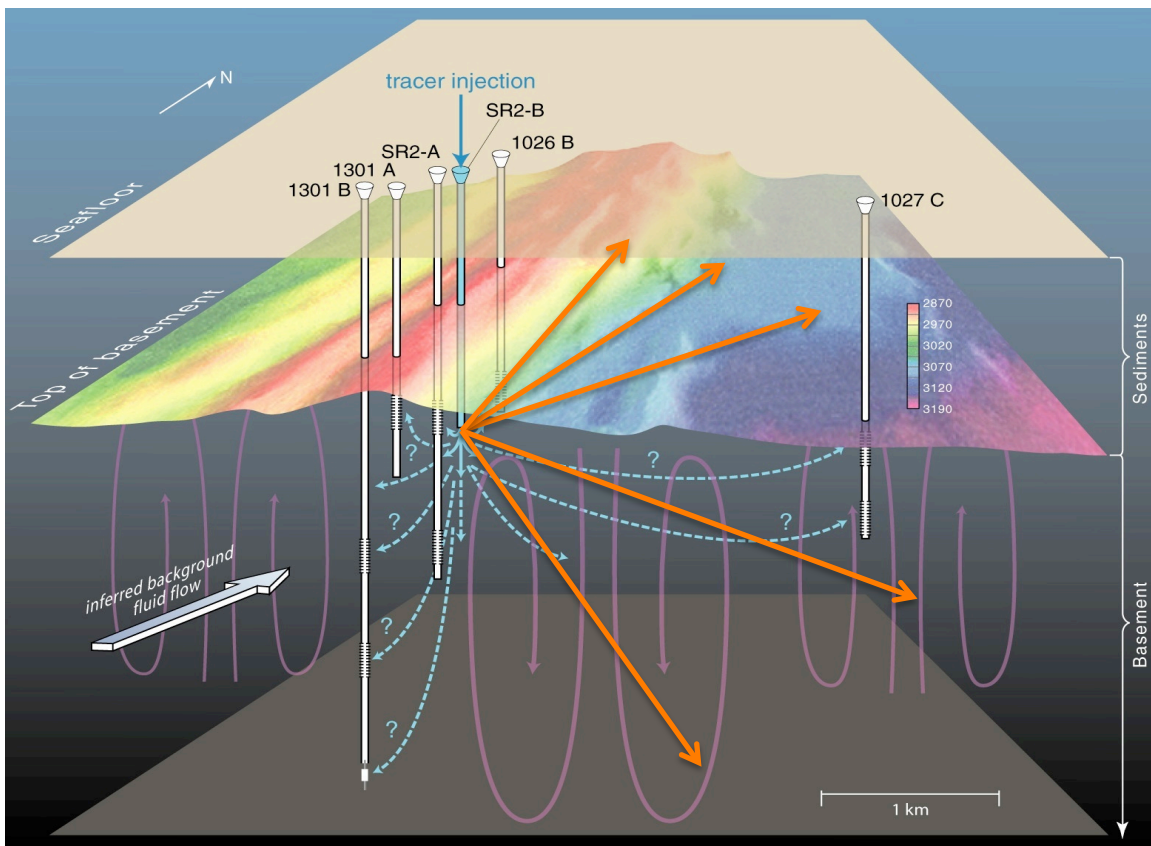


*Figure 20: Schematic of CORKs showing possible paths of tracer transport (orange arrows) that could potentially be undetected by continuous monitoring and sampling sites.*

# CHAPTER V
## CONCLUSION & FUTURE RESEARCH

Although much of the ocean floor is hydrogeologically active, very little is known about the physical properties of the ocean crust. The ocean basement contains a large volume of fluid, and the hydrological properties of this fluid flow influence the temperature and chemical state of these fluids, the transport of particles and solutes through the subseafloor ocean basement, and the formation and maintenance of microbial communities below the seafloor (Alt, 1995; Huber et al., 2006; Parsons and Sclater, 1977; Peacock and Wang, 1999).

Currently, there is little information regarding the flow paths of large-scale fluid transport in the oceanic crust. Scientific ocean drilling has long been in pursuit of obtaining a quantitative assessment of these physical properties in order to better understand the fluid-rock interactions in the subseafloor basement rock, as well as to better grasp tracer transport behavior in the upper ocean crust. The Tracer Transport Project has established a three dimensional network of pressure tight, subseafloor observatories. These observatories, or CORKs (Circulation Obviation Retrofit Kits), permit various disturbances associated with the drilling of boreholes and installation of CORKs (thermal, pressure, chemical) to disperse and allow for the collection of undisturbed, natural-state data. They can also function as long-term sites of sampling and monitoring (Davis et al., 1992).

Although microspheres injected at CORK U1362B have not reached the collection site at CORK U1301A, there are several possible explanations for their absence for 11 months of monitoring after injection. A likely explanation is that the microspheres are still in transit between the injection site and collection site, and they

simply have not arrived yet.  In order to test this hypothesis, continuous monitoring will

be necessary until their initial detection, which will be their time of arrival.  The samples

collected at U1362B showing a decrease in microsphere concentration by 7 orders of

magnitude indicate that the injected microspheres are indeed being transported elsewhere.

There are several possible explanations for this, and future sampling and sample analysis

is required for more conclusive results.

More information on the general direction of fluid flow and particle transport can

be gathered from the anticipated data because if the particles injected at U1362B are

eventually detected at a collection site, then that collection site must be in a down-

gradient location.

Further studies comprised of continuous CORK monitoring and analysis of

collected samples will be necessary to gain a complete quantitative understanding of the

physical properties in the upper ocean crust.  The GeoMICROBE sled will continue to

collect monthly samples from CORK observatories.  Each year, samples from the

GeoMICROBE are manually retrieved from the sites by crewmembers on the *R/V*

*JOIDES Resolution*.  These samples will be composed of whole fluids collected by the

GeoMICROBE, as well as filters that have undergone in-situ filtrations by the

GeoMICROBE instrumented sled.  CORK observatories are located at sites 1026B,

1027C, 1301A, 1301B, 1362A as well as the tracer injection site, 1362B.  Along with

continuous fluid sampling, other data to be logged will come from pressure monitoring,

temperature monitoring, and microbiological growth incubators.  Data gathered by these

monitors will help provide information about the biogeochemical conditions within the

upper ocean crust on the eastern flank of the Juan de Fuca Ridge.  These future studies

can benefit from the three dimensional network of CORK observatories that has been

established through the Tracer Transport Project.

# REFERENCES

Alt, J.C. 1995. Subseafloor processes in mid-ocean ridge hydrothermal systems. In Humphris, S.E., Zierenberg, R., Mullineaux, L., and Thomson, R. (Eds.), Seafloor Hydrothermal Systems: Physical, Chemical, Biological and Geological Interactions within Hydrothermal Systems. Geo- phys. Monogr., 91:85–114.

Altman, S. J., L. C. Meigs, T. L. Dones, S. A. McKenna. Controls of mass recovery rates in single-well injection-withdrawal tracer tests with a single-porosity, heterogeneous conceptualization, *Wat. Resour. Res.* 38, 1125 (2002).

Bach, W., S. E. Humphris, A. T. Fisher, Fluid flow and fluid-rock interaction within oceanic crust: reconciling geochemical, geological and geophysical observations in Subseafloor Biosphere at Mid-ocean Ridges. C. Cary, E. Delong, D. Kelley, W. S. D. Wilcock, Eds. (*American Geophysical Union*, Washington, D. C., 2004) pp. 99-117.

Bartetzko, A. 2005. Effect of hydrothermal ridge flank alteration on the in situ physical properties of upper- most oceanic crust. *J. Geophys. Res*., [Solid Earth], 110(B6):B06203–B06211. doi:10.1029/2004JB003228

Becker, M. W., A. M. Shapiro. Tracer transport in fractured crystalline rock: evidence of nondiffusive breakthrough tailing, *Wat. Resour. Res.* 36, 1677-1686 (2000).

Becker, M. W., D. W. Metge, S. A. Collins, A. M. Shapiro, and R. W. Harvey. 2003. Bacterial transport experiments in fractured crystalline bedrock. *Ground Water*, 41(5):682–689.

Birgersson, L., and I. Neretnieks. Diffusion in the matrix of granitic rock: Field test in the Stripa Mine, *Water Resour. Res.,* 26(11), 2833–2842, 1990.

Close, M. E., P. Liping, M. J. Flintoff, L. W. Sinton. Distance and flow effects on microsphere transport in a large gravel column. *J. Environ. Qual*. 35:1204-1212 (2006).

Cowen, J.P., Giovannoni, S., Kenig, F., Johnson, H.P., Butterfield, D., Rappe, M., Hutnak, M., Lam, P., 2003. Microorganisms in fluids from 3.5 m.y. Ocean Crust *Science*. 299, 120–123.

Cowen, J. P., B. T. Glazer, M. Rappe, A. Fisher, K. Becker, E. Davis, H. Jannasch, G. Wheat. 2006. "Microbial geochemical and tracer transport studies of ocean basement using ODP CORK observatories." *Geophysical Research Abstracts*. 8.10998.

Cowen, J.P, 2007 (Unpublished).  "NSF Project Description".

Cowen, J. P., D. A. Copson, J. Jolly, C. C. Hsieh, H. T. Lin, B. T. Glazer, C. G. Wheat. Advanced instrument system for real-time and time-series microbial geochemical sampling of the deep (basaltic) crustal biosphere. *Elsevier*,(2011).

Davis, E. E. and K. Becker. Using subseafloor boreholes for studying sub-seafloor hydrogeology: results from the first decade of CORK observations, *Geoscience Canada* 28, 171-178 (2002).

Davis, E. E., K. Becker, T. Pettigrew, B. Carson, R. MacDonald, CORK: a hydrologic seal and downhole observatory for deep-ocean boreholes, in *Proc. ODP, Init. Repts.* E. E. Davis, M. Mottl, A. T. Fisher, Eds. (Ocean Drilling Program, College Station, TX, 1992), vol. 139, pp. 43-53.

Davis, E. E. and H. Elderfield. *Hydrogeology of the Oceanic Lithosphere* (Cambridge University Press, Cambridge, UK, 2004), pp. 706.

Davis, E. E., A. T. Fisher, J. Firth. *Proc. ODP, Init. Repts.* (Ocean Drilling Program, College Station, TX, 1997), pp. 470.

Elderfield, H., and A. Schultz. 1996. Mid-ocean ridge hydrothermal fluxes and the chemical composition of the ocean. Annu. Rev. Earth Planet. *Science*. 24(1):191–224. doi:10.1146/ annurev.earth.24.1.191

Fisher, A. and K. Becker. 2000. Channelized fluid flow in oceanic crust reconciles heat-flow and permeability data. *Nature* 403: 71–74.

Fisher, A.T.; Cowen, J.; Wheat, C.G.; Clark, J.F., 2011. "Preparation and injection of fluid tracers during IODP Expedition 327, eastern flank of Juan de Fuca Ridge." *Proceedings of the Integrated Ocean Drilling Program*. 327.

Fisher, A. T., C. G. Wheat, K. Becker, E. E. Davis, H. Jannasch, D. Schroeder et al. Scientific and technical design and deployment of long-term, subseafloor observatories for hydrogeologic and related experiments, IODP Expedition 301, eastern flank of Juan de Fuca Ridge, in *Proc. IODP* A. T. Fisher, T. Urabe, A. Klaus, Eds. (Integrated Ocean Drilling Program, College Station, TX, 2005), vol. Expedition 301, pp. doi:10.2204/iodp.proc.301.103.2005.

Gillis, K.M., K. Muehlenbachs, M. Stewart, T. Gleeson, and J. Karson. 2001. Fluid flow patterns in fast spread- ing East Pacific Rise crust exposed at Hess Deep. *J. Geo- phys. Res*. [Solid Earth], 106(B11):26311–26329. doi:10.1029/2000JB000038

Gillis, K.M., and P. T. Robinson, 1990. Patterns and pro- cesses of alteration in the lavas and dykes of the Troo- dos ophiolite, Cyprus. *J. Geophys. Res*., [Solid Earth], 95(B13):21523–21548. doi:10.1029/JB095iB13p21523

Harvey, R. W., 1997. Microorganisms as Tracers in Groundwater Injection and Recovery Experiments: A Review. FEMS Microbiology Reviews 20. 461-472.

Huber, J. A., D. A. Butterfield, H. P. Johnson, J. A. Baross, Microbial life in ridge flank crustal fluids, *Environmental Microbiology.* 88, 88-99 (2006).

Integrated Ocean Drilling Program (IODP) Planning Sub-Committee (IPSC), "Earth, Oceans and Life, Initial Science Plan 2003-2013, Integrated Ocean Drilling Program," (International Working Group, 2001),

Johnson, H. P.; Pruis, M.J., 2003. Fluxes of fluid and heat from the oceanic crustal reservoir, *Earth. Planet. Science. Lett.* 216.

Karson, J.A., 1998. Internal structure of oceanic litho- sphere: a perspective from tectonic windows. In Buck, W.R., Delaney, P.T., Karson, J.A., and Lagabrielle, Y. (Eds.), Faulting and Magmatism at Mid-Ocean Ridges. Washington, DC (Am. Geophys. Union), 177–218.

Kenig, F., D. J. H. Simons, G. T. Ventura, D. Crich, J. P. Cowen, T. Rehbein-Khalily. 2005. Structure and distribution of branched-alkanes with quaternary carbon atoms in Cenomanian and Turonian black shales of Pasquia Hill (Saskatchewan, Canada). *Organic Geochemistry* 36 (1), 117–138.

Kenig, F., D. J. H. Simons, D. Crich, J. P. Cowen, G. T. Ventura, T. Rehbein-Khalily, T. C. Brown. 2003. Branched aliphatic alkanes with quaternary substituted carbon atoms in modern and ancient geologic samples. *Proceedings of the National Academy of Sciences (PNAS)* 100 (22), 12554–12558.

Mottl, M.J., 2003. Partitioning of energy and mass fluxes between mid-ocean ridge axes and flanks at high and low temperature. In Halbach, P.E., Tunnicliffe, V., and Hein, J.R. (Eds.), *Energy and Mass Transfer in Marine Hydrothermal Systems*: Berlin (Dahlem Univ. Press), 271–286.

Novakowski, K. S., The analysis of tracer experiments conducted in divergent radial flow fields, *Wat. Resour. Res.* 28, 439-447 (1992).

Novakowski, K. S., P. A. Lapcevic, J. W. Voralek, A note on a method for measuring the transport properties of a formation using a single well, *Wat. Resour. Res.* 34, 1351-1356 (1998).

Parsons, B., J. G. Sclater, An analysis of the variation of ocean floor bathymetry and heat flow with age, *J. Geophys. Res.* 82, 803-829 (1977).

Peacock, S.M., and K. Wang. 1999. Seismic consequences of warm versus cool subduction metamorphism: examples from southwest and northeast Japan. *Science*, 286(5441):937– 939. doi:10.1126/science.286.5441.937

Schulze-Makuch, D., Longitudinal dispersivity data and implications for scaling behavior, *Ground Water* 43, 443-456 (2005).

Skagius, K., and I. Neretnieks, Porosities and diffusivities of some nonsorbing species in crystalline rocks, *Water Resour. Res.*, 22(3), 389–398, 1986.

Underwood, M., K. D. Hoke, A. T. Fisher, E. G. Giambalvo, E. E. Davis, L. Zühlsdorff, Provenance, stratigraphic architecture, and hydrogeologic effects of turbidites in northwestern Cascadia Basin, Pacific Ocean, *J. Sediment. Res.* 75, 149-164 (2005).

Wheat, C.G., H. Elderfield, M. J. Mottl, C. Monnins. 2000. Chemical composition of basement fluids within an oceanic ridge flank: Implications for along-strike and across-strike hydrothermal circulation. *J. Geophys. Res.*-SolidEarth105, 13437–13447.

Wheat, C. G., H. W. Jannasch, M. Kastner, J. N. Plant, E. DeCarlo, Seawater transport and reaction in upper oceanic basaltic basement: chemical data from continuous monitoring of sealed boreholes in a ridge flank environment, *Earth. Planet. Sci. Lett.*, 549-564 (2003).

Wheat, C. G., H. W. Jannasch, A. T. Fisher, K. Becker, J. Sharkey, and S. Hulme. 2010. Subseafloor seawaterbasalt-microbe reactions: continuous sampling of borehole fluids in a ridge flank environment. *Geochem., Geophys., Geosyst.*, 11(7):Q07011. doi:10.1029/2010GC003057


Working Group 3. Fluid circulation in the crust and the global geochemical budget. Paper presented at the Second Conference on Scientific Ocean Drilling (COSOD II), Strasbourg 1987.

# APPENDICES

## Appendix A: Statistical t-test

First, obtain averages for each tower for each method. Determine the difference in measurements between methods (e.g. $direct_1 - stain_1 = di_1$). Now, find the average of these differences and the average measurement of diameter ($\bar{d}$ = average measurement of diameter). Find $di - \bar{d}$. Square the difference and then sum up all the squares. Determine the sample size n. For this case, n = 5 because there are 5 filtration towers. The mathematical equation describing the procedure for a statistical t-test is as follows:

$$SD = \sqrt{\frac{\sum(di - \bar{d})^2}{n - 1}}$$

It is also necessary to know the t-value for the given conditions:

$$t\text{-value} = \frac{\bar{d}}{SD} * \sqrt{n}$$

Look up the standard t-value in a t-table found online or any statistics textbook. From this table, determine the calculated experimented t-value ($t_{exp}$) and the statistical t-table value from the t-table ($t_{st}$). If $t_{exp} < t_{st}$, then the difference between the means obtained from the two different methods is statistically insignificant. If $t_{exp} > t_{st}$, then the difference between the means is statistically significant.

## Appendix B: Pipette calibration

The digital pipette had to be calibrated in order to verify its accuracy and precision. To do this, 1000μL, 500μL, and 200μL were pipetted into beakers and their respective masses were recorded (see Table 2). Ten trials of each volume were carried out, and then the whole procedure was repeated once. This provided twenty measurements of mass for each volume, although not all twenty of the measurements were done at the same time. The calculated level of accuracy is <1% from true accuracy, which is acceptable for the purposes of this experiment.

**Calibration done by pipetting 20 trials of three different volumes of DI water (ten 1000 µL, ten 500 µL, ten 200 µL then repeating each ten more times).**

| Mass (g) | mass (g) | mass (g) | |
|---|---|---|---|
| 1000 µL | 500 µL | 200 µL | |
| 1.0002 | 0.4956 | 0.1976 | |
| 0.9960 | 0.4961 | 0.1975 | |
| 0.9989 | 0.4954 | 0.1974 | |
| 0.9984 | 0.4954 | 0.1980 | |
| 1.0000 | 0.4947 | 0.1982 | |
| 0.9993 | 0.4953 | 0.1969 | |
| 0.9977 | 0.4959 | 0.1976 | |
| 0.9987 | 0.4943 | 0.1973 | |
| 0.9972 | 0.4942 | 0.1981 | |
| 0.9970 | 0.4951 | 0.1980 | |
| 0.9901 | 0.4956 | 0.1974 | ← **changed pipette filter** |
| 0.9888 | 0.4963 | 0.1982 | **tip after the first 30 trials** |
| 0.9896 | 0.4958 | 0.1978 | |
| 0.9882 | 0.4955 | 0.1975 | |
| 0.9879 | 0.4953 | 0.1974 | |
| 0.9888 | 0.4955 | 0.1980 | |

|  | | | |
|---|---|---|---|
|  | 0.9941 | 0.4956 | 0.1981 |
|  | 0.9933 | 0.4954 | 0.1986 |
|  | 0.9901 | 0.4943 | 0.1983 |
|  | 0.9897 | 0.4967 | 0.1988 |
| **Average** | 0.994 | 0.4954 | 0.1978 |
| **St. Dev.** | 0.004 | 0.0006 | 0.0005 |
| **RSD** | 0.4% | 0.1% | 0.2% |
| **True wt.** | 0.9977 | 0.499 | 0.200 |
| **%Accuracy** | **0.4%** | **0.7%** | **0.9%** |

*Table 2: The pipetted masses in this calibration data exhibit <1% variation from true accuracy, which is an acceptable level of accuracy for the purposes of this experiment.*

## Appendix C: Equation to make an appropriate concentration of acid

The necessary equation is as follows:

$$X = \frac{YC_2}{C_1} = \frac{(100 \text{ mL})(0.4\%)}{12\%} = 3.33 \text{ mL concentrated HCl}$$

X= amount of concentrated acid needed

$C_1$= concentration of concentrated acid

Y= amount of diluted acid desired

$C_2$ = desired concentration of diluted acid

Therefore, 3.33 mL concentrated HCl and 96.66 mL DI water (100 mL – 3.33 mL) are needed to reach the desired final concentration of 0.4% HCl.  These amounts were pipetted (always add acid to water!) into a glass beaker,

**Appendix D: Determining the density and total volume of a sample fluid**

       To determine the density and total volume of fluid in a sample (which is used when determining the concentration of microspheres in a fluid: number of microspheres/volume of filtered fluid), follow the procedure described here.  First, place a disposable cup on the scale and zero it out.  Pipette 1 mL of sample fluid into the disposable cup.  Record the mass (in grams) of 1 mL of sample fluid.  Repeat these steps (measuring the mass of separate 1 mL samples) at least five times, and calculate an average mass.  This value is the average density (units in g/mL).  Measure and record the mass of the remaining sample fluid and the bottle.

       Using the procedure described above (see section 2.2.0e), filter the entire bottle of sample fluid.  Measure and record the mass of the empty sample bottle.  Subtract the mass of the bottle and fluid from the mass of the bottle.  This will give the mass of the fluid that was filtered [(bottle + fluid) – bottle = fluid].  Now, multiply the reciprocal of the density by the mass of the fluid.  This will give the total volume of the filtered fluid:

$$\frac{mL}{grams} \; x \; grams = mL$$

## Appendix E: Ocular grid calibration

Calibrating the ocular grid for each objective lens in a microscope requires a slide micrometer (stage micrometer). The goal of this calibration is to be able to obtain an accurate scale of size for each different level of magnification. First, place the micrometer under the microscope as if it were a sample slide. Line up the left tick mark of the micrometer with the left border of the ocular grid. Then find the farthest-right instance where the two (grid tick mark and micrometer tick mark) overlap perfectly. Divide the number of micrometer tick marks by the number of ocular grid lines (ie. 88/9 = 9.78). This gives the number of micrometer lines per grid line. The fact that the entire micrometer is 1.00mm with 0.01 mm increments must also be taken into account. To do this, multiply the quotient (ie. 9.78) by 0.01 mm to get the answer in units of mm. To convert this to μm, simply multiply the number by 1000. This will give the length of one tenth of the side of the ocular grid. In between trials, align and realign the grid and micrometer. Also, with higher magnification, some perfection in alignment is lost. When this happens, simply make the best possible estimates.

| Eyepiece | Trial | Micrometer | Ocular Grid | μm lines/O.G. line | Observer |
|---|---|---|---|---|---|
| 10x | 1 | 88 | 9 | 9.78 | Jim |
| | 2 | 78 | 8 | 9.75 | Jordan |
| | 3 | 59 | 6 | 9.83 | Tina |
| 40x | 1 | 24.8 | 10 | 2.48 | Tina |
| | 2 | 19.8 | 8 | 2.48 | Jordan |
| | 3 | 14.9 | 6 | 2.48 | Jordan |
| 100x | 1 | 9.9 | 10 | 0.99 | Jordan |
| | 2 | 10 | 10 | 1.00 | Jordan |
| | 3 | 9.9 | 10 | 0.99 | Jordan |

*Table A: Data for calibration of ocular grid on epifluorescence microscope.*

| Eyepiece | Average (μm lines/O.G. line) |
|---|---|
| 10x | 9.79 |
| 40x | 2.48 |
| 100x | 0.99 |

*Table B: Shows average number of micrometer lines per ocular grid line.*

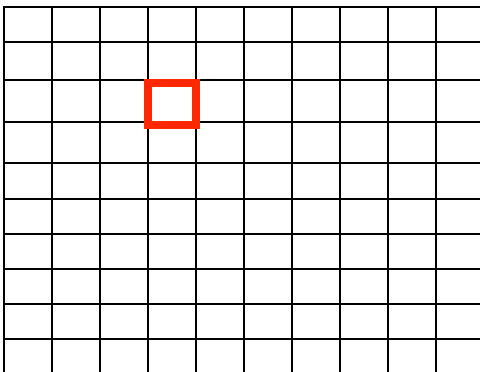**Conversions:**

**following are lengths for the side of one L1 x L1 square in the ocular grid**

For 10x magnification:  9.79 (μm lines/O.G. lines) x (0.01 mm) = 0.0979 mm = 97.9 μm

For 40x magnification:  2.48 (μm lines/O.G. lines) x (0.01 mm) = 0.0248 mm = 24.8 μm

For 100x magnification:  0.99 (μm lines/O.G. lines) x (0.01 mm) = 0.0099 mm = 9.9 μm



*The entire ocular grid is 10(L1) x 10(L1) meaning each box has an area of L1 x L1. The lengths above represent the length of L1 for the corresponding ocular magnification.

**RED** = L1 x L1